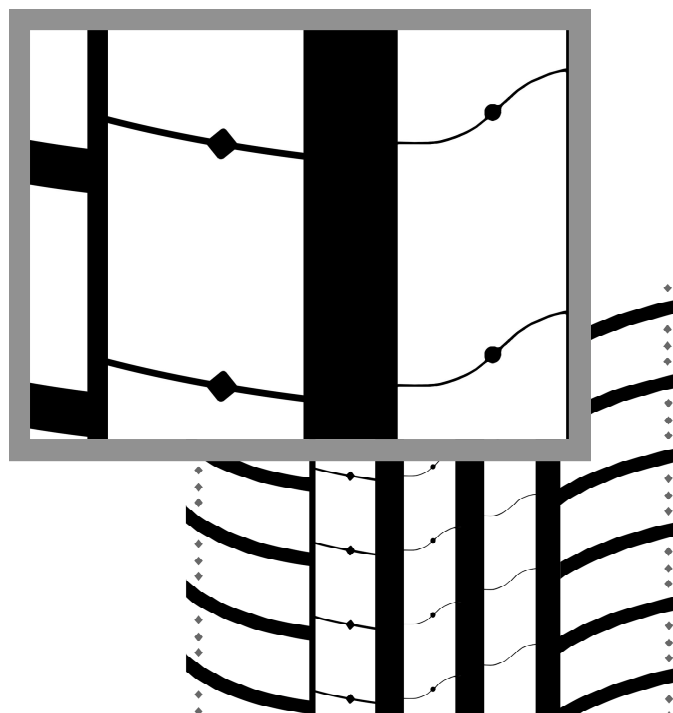


# CHALMERS



## Visual and acoustic tyre tread design

Master's Thesis in the International Master's programme Sound and Vibration

**KARIN LILJEGREN**

Department of Civil and Environmental Engineering  
*Division of Applied Acoustics*  
*Vibroacoustics Group*  
CHALMERS UNIVERSITY OF TECHNOLOGY  
Göteborg, Sweden 2008

Master's Thesis 2008:118  
ISSN 0283-8338

<b>1. INTRODUCTION.....</b>	<b>2</b>
<b>2. TYRE TREAD.....</b>	<b>3</b>
2.1 TYRE/ROAD NOISE .....	3
2.2 TYRE & TREAD .....	3
2.3. TYRE TREAD EVALUATION SOFTWARE.....	6
<b>3. VISUAL DESIGN .....</b>	<b>19</b>
3.1 DESIGN FORMAT ANALYSES .....	19
3.2 FORMULATING GUIDELINES AT CONTINENTAL .....	19
3.3 FUNCTIONS MATRIX AND PRODUCT SPECIFICATION .....	20
3.4 EXPRESSIONS AND CONCEPT GENERATION .....	21
3.5 CONCEPT RESULTS.....	22
3.6 CONCEPT EVALUATION.....	23
<b>4. ACOUSTIC DESIGN .....</b>	<b>24</b>
4.1 PATTERN ALTERATION PROCEDURE.....	24
4.2 CONTROLLED VOID CONTENT .....	24
4.3 LARGER ANGLE OF SHOULDER GROOVES .....	26
4.4 WIDTH OF SIPES .....	28
4.5 S-PATTERN SIMULATIONS .....	29
4.6 BASIC PATTERNS .....	32
4.7 RANDOMIZATION.....	35
4.8 CROSS BARS WITH DECREASING GROOVE WIDTH BUT CONSTANT VOID AND BLOCK REPETITION .....	37
4.9 SHIFTS .....	39
4.10 SHIFT ON PATTERN 2.....	42
4.11 MOVING VOID.....	43
4.12 IMPROVING PATTERN 2 BY COMBINING METHODS .....	44
<b>5. DISCUSSION .....</b>	<b>47</b>
<b>6. CONCLUSIONS .....</b>	<b>48</b>
<b>7. REFERENCES.....</b>	<b>50</b>
<b>APPENDIX I – DFA .....</b>	<b>51</b>
<b>APPENDIX II – FUNCTIONAL MATRIX AND PRODUCT SPECIFICATION .....</b>	<b>54</b>
<b>APPENDIX III - QUESTIONNAIRE .....</b>	<b>55</b>
<b>APPENDIX IV – EXPRESSION EVALUATION RESULTS .....</b>	<b>56</b>

# 1. Introduction

## Background

With increasing demands and in times of tougher competition, visual qualities often come through as a highly competitive means. Tyres are no exceptions. Marketing of a tyre today lies not only in proving its functional qualities, but also in fulfilling aesthetic requirements. The importance of visual design has grown also in this field.

Tyre manufacturers today are also under pressure to deliver quiet tyres, complying to maximum sound levels [5]. Both increased traffic volumes and awareness of increased noise pollution, makes the subject of sound design of tread essential. Of all parts of a tyre, the tread is unquestionably the most influential on the tyre/road noise. The tread design is responsible for the distribution of forces on the contact patch, and the visual tread design therefore stands in immediate connection with the sound emission. The tread design also directly influences many other qualities of the tyre, and the fascination of these connections, especially between visual and acoustic design, was the incentive for this thesis topic.

Much work has been done at the department of Applied Acoustics at Chalmers University of Technology, to model the sound mechanisms that originate from the tyre/road interaction. In this thesis work a model, which has previously been developed and used at the faculty for evaluating road surfaces, has been used to simulate the radiated sound levels from the developed tread patterns.

## Problem definition

In this thesis work the following questions were set out to be answered:

What is the connection between visual and acoustic tyre tread design?

What are the limitations for realistic visual tread design?

How does tread design affect sound emission?

What role does the tyre stiffness play to sound emission in SPERoN software simulation?

What are the possibilities and limitations in using the SPERoN software for evaluating tread pattern designs?

## Purpose

There are several purposes for this thesis. One is to find tyre tread design intended for a specific customer and company. Another purpose is to show the possibilities and limitations of tyre tread designs, which have the demands of a normal tyre on them. Yet another purpose is to investigate tread design features from the acoustic point of view, in order to reach improved understanding of how to achieve tread designs with sought sound qualities. Finally, the purpose is also to investigate and evaluate the usefulness of the software SPERoN for simulations of tread designs.

## Aim

This thesis work aims to give a simple overview of the possibilities and limitations in the complex relation between visual and acoustic tread design. It also aims to show how certain changes in design influences the sound emission, especially through influencing the tyre

stiffness. This thesis also aims to generate general guidelines, and to create concept patterns from those. It further aims to evaluate some of the guidelines from the simulation results. For Continental and for Chalmers this thesis will also result in knowledge about using the software SPERoN for simulating sound emission from tyre/road interaction in evaluating tyre tread patterns.

### **Delimitations**

The fourth generation in the series CSC (Continental Sport Contact) was under development and was selected as a basis for this work. This tyre was suitable since it had already been under development for some time, and many decisions regarding its mechanical qualities already had been set. As an Ultra High Performance tyre, this tyre is intended for extreme sports cars and for use in summer, mainly on tarred and concrete roads.

The simulations required a large amount of input tyre data. This is not easily acquired, which is why a collection of data which was already available was used. Based on another tyre by Continental, the Continental Premium Contact, this data somewhat misrepresents the material and constructional data of the new tyre. However, being a popular summer tyre from the same manufacturer there are also many similarities. Furthermore, relative and qualitative comparisons between results should still be valid.

## **2. Tyre tread**

### **2.1 Tyre/road noise**

Tyre/road noise mechanisms are often divided into two groups, due to their origin. Mechanisms from the first group are directly linked to mechanical vibrations and are therefore structure bound. To this group belong various impact and adhesion mechanisms of the tyre.

The second group consists of aerodynamic phenomena such as air pumping. Varying amplification processes for the generated sound, e.g. pipe resonances, (originating from the cavities and geometries around and between tyre and road and within the tyre construction) add to these sound mechanisms [2]. In the simulations for this thesis emphasis is on the over all sound levels, i.e. the emission from all these sources together.

### **2.2 Tyre & tread**

A passenger car tyre today is normally of radial type, which means that the cords of the carcass construction are placed in the radial direction. The terminology of the different parts and definition of directions are shown in Figure 1 and 2 below.



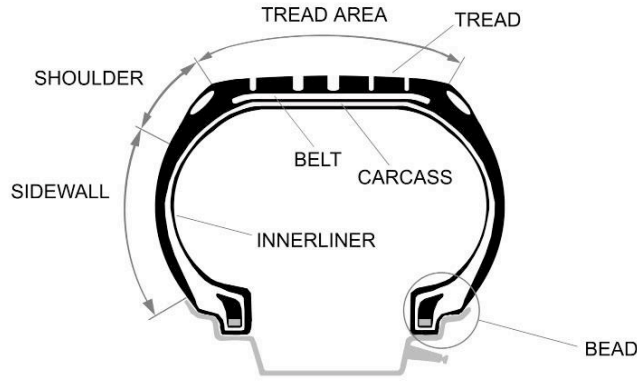


**Figure 1.** Tyre section

The typical passenger car tyre as indicated in the picture contains several materials, built up in layers made of elastomers, metal and textile reinforcements to give it the right mechanical qualities [3]. However, the tyre tread is made of rubber compounds, which are incompressible, which means that compression in one place involves expansion elsewhere [3]. Further the stiffness of the material increases with the compression.

The reference terms for directions are commonly longitudinal (x), transversal (y) and vertical (z) [3]. Since this thesis focuses on tread design, the terms **radial** (z), **horizontal** (y) and **circumferential** (rotating around the z axis) have instead been used.



**Figure 2.** Reference directions.

The contact patch between tyre and ground is called the footprint (figure 3). The size, shape and design of grooves within this patch largely influence the tyre performance. Any grooves outside of it contribute to air turbulence noise, which is a very small part of the total sound emission, but dominant at very high frequencies. The footprint measure PB (figure 3) describes the width of the whole tread pattern. The measure  $TW_{45}$  describes the width within which the tread has a chance of being in contact with the ground [4]. The rubber of the tread and the sidewall of the tyre meet at the split line. For this thesis patterns were created for the area within PB, knowing that the area outside  $TW_{45}$  is not in contact with the ground and therefore neither will have a large impact on tyre performance nor on sound emission in the

simulations. For each pattern the area outside  $TW_{45}$  was also removed before processing it in Matlab for the simulations.

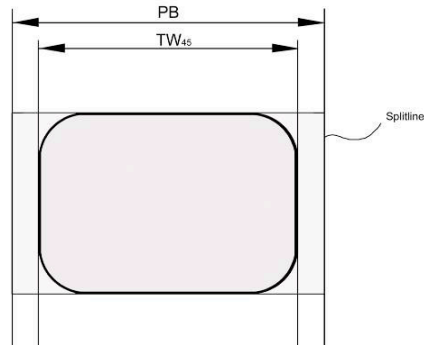


**Figure 3.** Typical, simplified footprint shape (dark area).

The footprint is dependant on many things, such as tyre construction and materials, inflation pressure and vehicle load. These parameters have all been kept constant for this thesis.

### Tread terminology

**Grooves** are basically anything that is “hollow” in the tread. The term **sipe** is used for grooves that are very thin, the smallest cuts in the rubber. These make the tread softer and are used extensively in winter tyres, especially in so called friction tyres, intended for icy conditions [8].

**Circumferential grooves** are sometimes called aqua lines, since these have a very important function on wet roads, where they enable contact with the ground. They are usually thick grooves extending around the whole tyre circumference. The **shoulder blocks** are the outmost/innermost chunks of rubber that are in contact with the ground and are created from many grooves placed circumferentially around the tyre, and running horizontally across the shoulders, out to the area where the blocks are no longer in contact with the ground. (Figure 1 shows the shoulder area as not being in contact with the ground. However, the shoulder blocks begin in the area denoted tread area in this figure, and are therefore always partly in contact with the ground.) The length of a shoulder block may further be called **pitch length**.

Patterns that have only horizontal grooves are called **cross bars**. A tyre with no tread pattern is called a **slick tyre** and is what is used on Formula 1 cars. Apart from this exception, these two types are only used for research purposes.



**Figure 4.** Tyre tread terminology

### **Template of grooves**

At Continental several departments had worked together in teams to find the right characteristics of the new product so that it would fulfil its product specification. One decision that had been made was the layout of the circumferential lines, which should stay close to certain dimensions in order to actually pass these requirements. The general template (figure 5) constituted the template for the initial concept patterns for this thesis. Letting the designs stay close to this was a key in giving the tyre tread the desired characteristics, especially regarding water handling.



**Figure 5.** The circumferential grooves, which were the basis for all concept patterns.

## **2.3. Tyre tread evaluation software**

### **SPERoN software – a prediction tool for pass-by measurements**

The generation of noise due to tyre/road interaction is complex process with several source mechanisms involved. In general two main mechanisms can be distinguished, tyre vibrations and air-flow related mechanisms such as air-pumping.

Tyre vibrations occur due to any disturbance leading to time varying contact forces exciting the tyre to vibrations, which are then radiated to the surrounding. Such disturbances can be the roughness of the road surface, the tread profile or varying properties of the tyre structure.

Air flow related mechanisms arise due to the displacement of air which is caused by changes in the contact geometry (e.g. closing and opening of cavities, deformation of the tyre tread, etc). The displacements or more exact, the acceleration of air leads to this generation of sound.

As a consequence of their different characters, tyre vibrations and air-flow related mechanisms have different driving speed dependency. Both mechanisms are present over the

whole frequency range, however tyre vibrations dominates at lower frequencies (typically below 1 kHz) while air-flow related mechanisms dominate at higher frequencies (above 1kHz).

The SPERoN prediction tool was created to predict pass-by levels including both mechanisms as well as aerodynamic noise from the vehicle and, for certain cases, also noise radiated from the tyre cavity (i.e. the space between tyre structure and rim). In order to accomplish this, a combination of two models, the so called “contact model” and a statistical tyre model was used to form what is later referred to as the “hybrid-approach”.

For the first mentioned part of the hybrid approach, the contact model, the contact forces are calculated as a function of

- dynamic properties of the tyre,
- road roughness,
- tread stiffness,
- tread profile,
- tyre load and
- driving speed

The contact forces are then allowed to constitute the input parameters to the other half of the hybrid model, the statistical model. In the statistical model

- contact forces,
- tread stiffness,
- tyre width and
- driving speed

have been related by coefficients and exponents to a vast data base of measurements collected in the German “Sperenberg” project.

In this chapter the construction of SPERoN as a prediction tool for tyre/road noise and as a function of tread design will be discussed. Some of the potentials and weaknesses will also be explained. In later chapters in this thesis further discussions around potentials and weaknesses of the SPERoN software in this usage will be developed in discussions, and will be related to discoveries made during the performed simulations and practical examples.

### **The contact model**

There are many different ways of designing prediction models for tyre/road interaction forces. The main idea of the SPERoN software was not to find a perfect tool for optimising tyre design or for basic research of noise generation mechanisms. Instead the tool was developed with the following purposes:

- Constituting a quick prediction tool for engineers wanting to find out the influence of road surface properties on the generated noise for an assembly of tyres and as a function of rolling speed.

- Delivering contact forces as function of road texture, in order to supply a statistic model with a linearized input.

Predicting the contact forces for a multitude of different tyres, being representative for typical traffic composition, on the road surface. (Material data are not available from the tyre manufacturer for these tyres. This means that the tyre models used in the approach have to have sufficiently accurate, while at the same time of enough complexity for the required input data to be able to be extracted from measurements of these tyres.)

Coping with a description of the road textures profiles which is accurate enough for the purpose. (These generally have to be a compromise between required information and what is feasible to measure.)

Providing a fast prediction model based on a multitude of calculations, since speed, surface texture, tyre and load variations demand a vast number of calculation cases.

Based on these requirements the following properties were decided on for the contact model:

- Application of simplified tyre models for the pre-calculation of the impulse response functions

- Consideration of a full 3 dimensional contact in a simplified way based on non-linear stiffness functions representing the lateral roughness distribution of the road texture.

- Decoupling of radial and tangential contact forces

### **The main structure of the contact model**

This module consists of two sub modules, the tyre model and the contact model. The tyre model calculates the required impulse response functions from collected measurements and these impulse response functions are then used in the contact model.

The contact model has the task of solving the non-linear problem of the contact between a particular tyre and a particular road. In this way the problem is made simpler since it can be split into two parts. The use of the pre-calculated impulse response functions reduces the numerical effort substantially compared with, for instance, Finite Element methods. This approach also allows for treating the tyre model and the contact models separately. In this way one can always use the model with the most appropriate features with respect to complexity, numerical efficiency, accuracy, etc. In the following the modelling of the tyre structure is described.

Beside this a pre-processing of data is also needed. This concerns extractions of the main tyre data from measured point mobilities and the preparation measurements of the road surface textures for the contact module, which is also described below.

### **Tyre model**

In the tyre model the tyre has been simplified to an orthotropic plate on an elastic foundation (springs). This simplification has the advantages of being both easy to handle and of being sufficiently accurate in frequency ranges up to 4 kHz. (The two sidewalls and the belt are thought to form a flat plate with different bending stiffness in the longitudinal and lateral directions (see Figure 6).

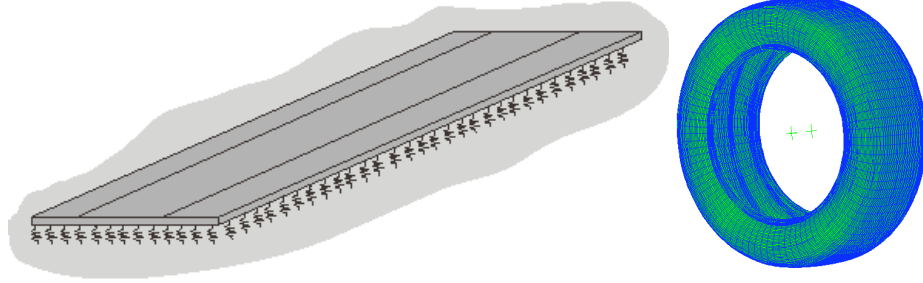


**Figure 6.** Simplified geometry of the orthotropic plate model. Sidewalls and tread build one flat plate. The support by inflation pressure and sidewalls are simulated by an elastic bedding.

The differential equation for the vertical motion of a plate is:

$$T_0 \left( \frac{\partial^2 \xi}{\partial x^2} + \frac{\partial^2 \xi}{\partial y^2} \right) + B_x \frac{\partial^4 \xi}{\partial x^4} + B_{xy} \frac{\partial^4 \xi}{\partial x^2 \partial y^2} + B_y \frac{\partial^4 \xi}{\partial y^4} + m^* \frac{\partial^2 \xi}{\partial t^2} + K \xi = F_0^*$$

The plate is under the tension  $T_0$ , which is caused by the interior air pressure of the tyre and which has the bending stiffness  $B_x$  in the circumferential direction and the bending stiffness  $B_y$  in lateral direction.  $B_{xy}$  is the cross stiffness and can well be approximated by  $B_{xy} \approx \sqrt{B_x B_y}$ .  $\xi$  is the vertical displacement and the radial displacement in the co-ordinates of the tyre. The elastic foundation of the belt is represented by the spring stiffness  $K$ .  $m^*$  is the mass per cross section and  $F_0^*$  is the acting force per cross section. A modal approach is used to solve the equation.

Comparisons of the model with measurements show a surprisingly good agreement as long as:  
the excitation area is not too small - otherwise the local stiffness becomes involved and this is not included in the model  
one has an accurate set of material parameters for the tyre and a very exact representation of these in this model.

#### Shortcomings of the tyre model:

The shift of the resonance frequencies for the range below the ring frequency. The shift is caused by the neglecting of the circumferential curvature of the real life structure. However this shift can be compensated by frequency dependent material parameters.

Similar problems occur due to neglecting the lateral curvature but can be cured in the same way.

The model can only be used up to about 4000 Hz, since at this frequency the thickness  $h$  of the plate is comparable with the wavelength of the bending waves and the bending wave model ceases to be representative, while other wave types start occurring here.

Despite these shortcomings the model of the orthotropic plate is a simple and useful tool to describe the structure-borne sound properties of a tyre with a low numerical effort.

#### Input data for tyre model

A big advantage of this tyre model is the limited number of input data required to run the model. These data are:

Mass per unit area of the tyre structure  
Bending stiffness (radial) depending on the inflation pressure and the sidewall stiffness  
Tension: depending on the inflation pressure  
Circumferential bending stiffness  
Lateral bending stiffness  
Damping. (This has to be determined as complex modulus for the different stiffness terms.)

### **Modelling the tread**

One of the important features of the SPERoN model is that it is suitable to capture the individual tyre properties, i.e. it can be used to predict the performance on individual tyres on different road surfaces. For this purpose, the following tyre tread input data are also needed:

Hardness of the tyre tread  
Tread profile

### **Hardness**

The hardness of the tyre is normally measured at three different places, two positions on the sidewall and one on the tread. The value measured at the tread is used as input into the contact model. This type of measurement is very much dependent on the procedure of measuring. Therefore the values are not used as absolute values but as a scaling factor related to a reference value (i.e. the value used when establishing the statistical model).

### **Tread profile**

The stiffness of the tread is not only determined by the elasticity of the tread compound, but also by the tread pattern. For this reason, the tyre tread pattern is normally measured in 3 dimensions with a laser scanner but in this project a picture file was used instead.

From these two types of information the total stiffness for each circumferential position of the tyre is calculated.

The main idea in the contact model is that the circumference is divided into a number of discrete slices across which the contact varies depending on the road roughness distribution and on the tread profile. Figure 7 (**upper left corner**) shows the profile for the first 150 slices (typically the circumference is divided into 750 or 1024 slices). Figure 7 (**upper right corner**) shows these slices and a straight, blue horizontal line. For each slice the area above the horizontal line is calculated. The idea is that the tyre is running only on this area. One could call it the visible profile during rolling as shown in Figure 7 (**lower left corner**). The area above the horizontal blue line gives a normalised stiffness curve for the tread. (This stiffness would be equal to one (1) if the tyre were to be a slick tyre.)

The variation of the stiffness along the circumference as shown in Figure 7 (**lower right corner**) represents the excitation of the tyre due to the variations in tread profile. The variation of the stiffness function  $p_m$  represents an excitation of the tyre exactly as the roughness of the road texture.

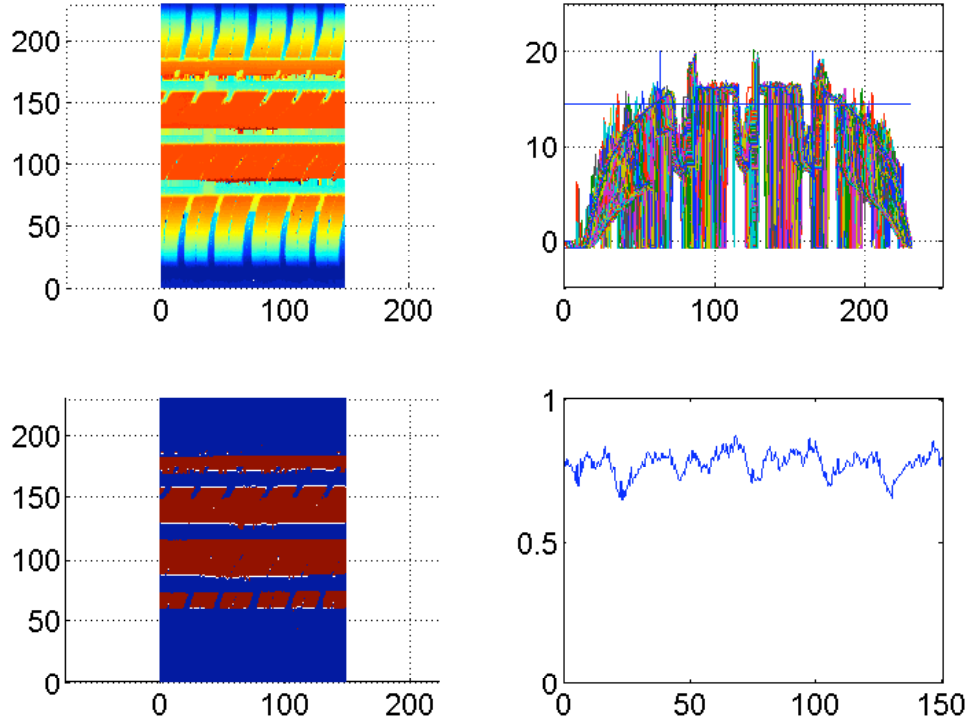


**Figure 7.** Extracting the tread profile stiffness. **Upper left corner:** measured profile by means of a laser scan for the first 150 slices. **Upper right corner:** the 150 slices in profile indicating the amount of rubber being in contact during rolling (i.e. the area above the blue horizontal line). **Lower left corner:** profile which is visible during rolling (red). **Lower right corner:** Variation  $p_m$  of the normalized tread stiffness due to the tread profile.

### Contact model

The problem to describe the contact between tyre and road may be studied at different scales. The fundamental elements of surface physics are the bonds between atoms or molecules that may be strong (ionic, covalent or metallic) or weak (hydrogen or van der Waals) and are all due to electromagnetic force. In a solid or a liquid these are the bonds that must be broken in order to create a new surface. Such models haven not been used in the simulation of tyre/road noise generation.

At a larger scale the interaction of elastic bodies can be studied by applying models like contact stiffness or friction coefficients having their origin in the physics behind the interaction of molecules. It is this scale for which today's contact models in SPERoN are mainly formulated.

As a first starting point one could think about the tyre as a structure where a Winkler bedding is added (i.e. a model of isolated springs). These springs represent the local contact stiffness due to the interaction between the road surface and the rubber tread of the tyre. The contact forces at any point in the contact are consequently given by the stiffness of the bedding and its compression. The compression of the spring  $\Delta y_e(\varphi_e, t)$ , at the angle  $\varphi_e$  is a function of the centre of the rim  $y_0(t)$ , the curvature  $k_2(\varphi_e)$  of the tyre, the vibration  $\varphi_e(\varphi_e, t)$  of the tyre belt and the roughness  $k_{10}(\varphi_e, t)$  of the road.

$$\Delta y_e(\varphi_e, t) = y_0(t) + k_{10}(\varphi_e, t) + \xi_e(\varphi_e, t) - k_2(\varphi_e)$$

The contact force is then



$$F_e(\varphi_e, t) = s\Delta y_e(\varphi_e, t)H[-\Delta y_e(\varphi_e, t)]$$

where  $H$  is the step function switching contact on and off depending on  $\Delta y_e(\varphi_e, t)$ . Since the motion of the tyre is a function of the forces, a non-linear equation system has to be solved for each time step in order to obtain the contact forces.

$$\xi_e(\varphi_e, t) = \sum_{m=1}^M F_m(\varphi_m, t) * g_{m,e}(t)$$

$g_{m,e}(t)$  is the impulse response function of the tyre structure at position  $e$  due to an impulse at position  $m$ . The implementation in the time domain allows for considering non-linear stiffness for the contact or relaxation for the rubber material. In such a model only contact forces normal to the surface are considered. This so-called “quasi three dimensional contact model” has been developed for the SPERoN approach.

The main idea is that when a piece of rubber is pressed on a rough surface, the resulting contact force will be proportional to the rubber area in contact with the rough surface as shown in Figure 8.

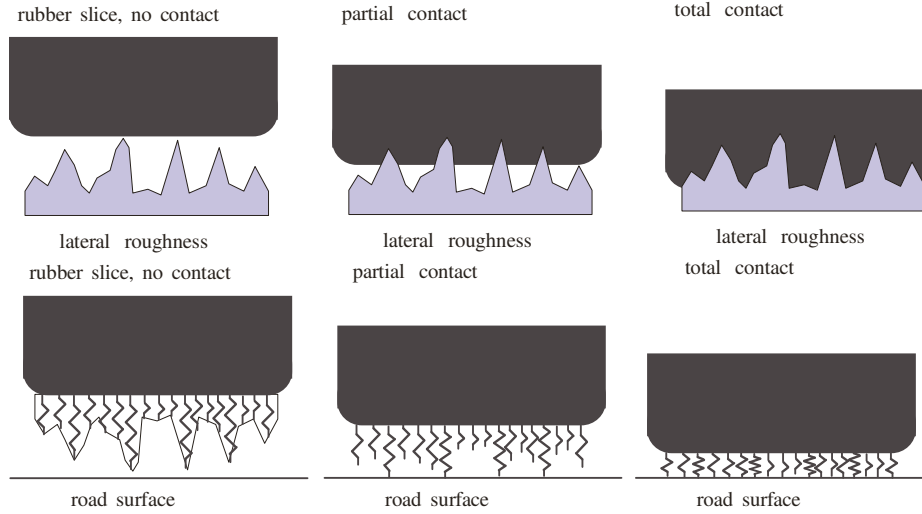


**Figure 8.** Schematic presentation of a lateral rubber slice in no, partial, and total contact with the road surface (upper figure) and realization as a Winkler bedding (lower figure).

This will lead to a non-linear stiffness depending on the lateral roughness distribution of the road surface. The resulting contact force  $F(t, \varphi_e)$  is now

$$F(\varphi_e, t) = \int_0^{\Delta y_e(\varphi_e)} s_e(\eta) d\eta$$

where  $\Delta y_e$  is the indentation depth and  $s_e$  is the stiffness function. In this way the lateral roughness pattern of the road is translated into a variation of the characteristic function of the non-linear bedding stiffness. For each slice of the tread such a characteristic function is calculated. In this way the circumferential variation of the roughness including the lateral characteristics of this change is taken into account. This is no severe complication of the previous model since the values of the integral can be pre-calculated and interpolation routines can be used to read values in between pre-calculated ones. The values are represented by the function  $K(\Delta y_e)$

Figure 9 (left) shows a typical roughness distribution over the width of the tread and as function of the ‘slice’ number (in this case the circumference is divided in 512 slices

corresponding to 3.4 mm width of each slice). On the right hand side of the figure the corresponding stiffness function are displayed.

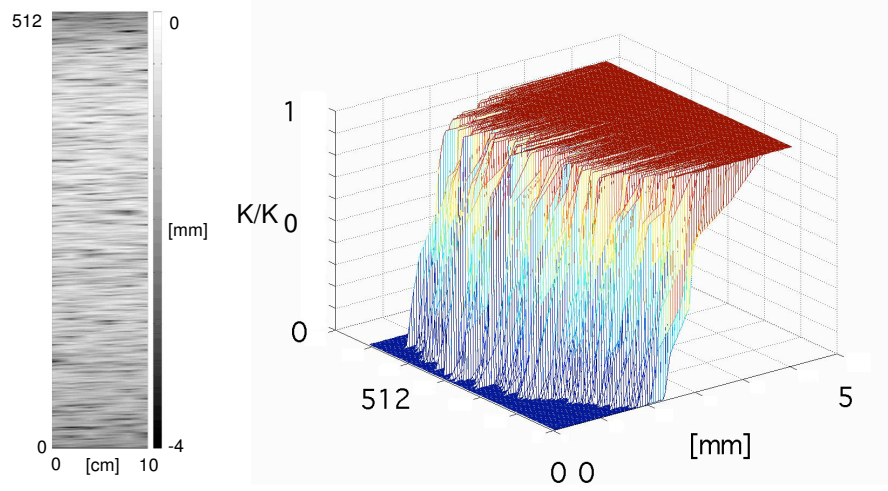


**Figure 9.** Examples of a 3D roughness pattern and the corresponding stiffness of the bedding (normalised by the stiffness for total contact over the width of the tyre)

The stiffness  $K_0$  represents the tread stiffness of the tyre. This quantity is measured for each individual tyre involved in the model (see previous text).

The roughness is measured in six parallel tracks, which has shown that it is a sufficient statistical description of the road texture as long as the texture is not an artificially created texture with strong anisotropy. However, in this case the number of measured tracks can be increased to ensure a good description of the lateral roughness distribution.

The contact forces in each position “m” on the tread are given by the product

$$F_m = K_0 \alpha p_m K(\Delta y_m)$$

where  $K_0$  is a standard value for a slick tyre (reference value),  $\alpha$  a correction factor for the hardness of the tyre,  $p_m$  a function taking into account the stiffness variation of the tread due to the pattern and  $K$  the roughness caused stiffness variation (i.e. different area in contact as function of the road roughness indenting the tyre)

From the simulations contact forces can be obtained as shown in Figure 10. The plot shows the total normal contact force as function of time. The first part is the loading process. Then the tyre starts to roll. After a few revolutions the tyre reaches a “steady state condition” and the contact force is only a function of the roughness variation in the contact. The results are shown for a surface from the Sperenberg project and for a rolling speed of 80 km/h.

The last part of the total contact force (150 ms, i.e. the small box in the right upper corner) is then used to calculate the contact spectra.

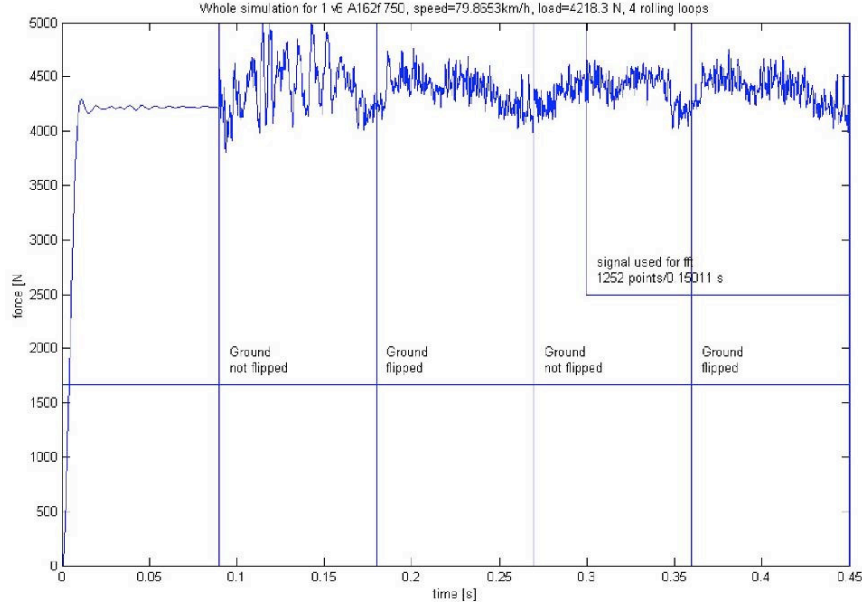


**Figure 10.** Total normal contact force as function of time for a surface from the Sperenberg project at a speed of 80 km/h. The last part of the total contact force (150 ms, i.e. the small box in is then used for the evaluation of the contact force spectra.

The calculated contact spectra are input into the he statistical model, described in the following.

### A statistical model for the pass-by situation

As described in the previous text there are a several mechanisms which contribute o the pass-by levels. In the statistical model the following mechanisms are taken into account:

**tyre vibrations**  $p_{vibration}^2$  representing the mechanical excitation of the tyre by the tyre profile and the road roughness

**air-flow related noise**  $p_{air-flow related}^2$  due to displacement of air in the vicinity of the contact between tyre and road

the **radiation from interior resonances** of the cavity between tyre structure and rim  $p_{cavity}^2$

and the **aerodynamic noise from the vehicle**  $p_{aerodynamic}^2$ .

The contribution from all source terms is additive (i.e. they are assumed to be uncorrelated)

$$p_{pass-by}^2 = p_{vibration}^2 + p_{air-flow\ related}^2 + p_{cavity}^2 + p_{aerodynamic}^2$$

For each of the source terms, coefficients and exponents have to be determined. In the following the different terms are discussed more in detail.

### Tyre vibrations

This term is mainly based on the pre-calculated contact forces  $F_c$  that lead to an excitation of the tyre structure and a radiation of sound. The radiation is strongly dependent on the horn effect and therefore on the properties of the road surface characterised by the flow resistance  $\Gamma$  and the tyre width  $B$ . It turned out that there is also a dependency on the tread stiffness  $S$ . The strong dependency on the tyre width and tread stiffness was mainly obvious in the frequency range around 400 -800 Hz. It is the range where the horn effect starts to act (see figure below). Increasing tyre size will lead to an earlier “start” of the horn effect. This increase can be substantial and therefore it has to be considered in the statistical model for both tyre vibrations and air-flow related effects.

The expression for this term is

$$p_{vibration}^2 = a F_c^2 \Gamma^{\alpha_1} B^{\alpha_2} S^{\alpha_3}$$

, where  $a$  is the coefficient and  $\alpha_1, \alpha_2, \alpha_3$  are exponents determined by the statistical model.

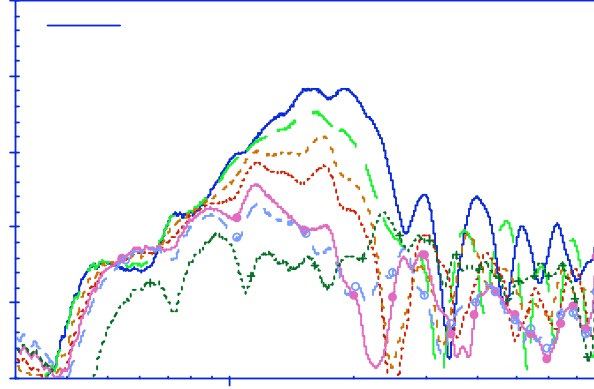


**Figure 11.** Amplification due to the horn effect for the different directions

### Air-flow related noise

The air-flow related noise includes all effects which lead to a displacement of air from the vicinity of the contact between tyre and road. This is represented by the ratio of contact force and contact spring leading to an averaged indentation between tyre and rough road surface. The exponent for the driving speed  $U$  is fixed to “4” as for monopole sources. The dependency of the radiated sound on the horn effect and in this way on the tyre width is included in the same way as for the tyre vibration contribution. The approach for the contribution of air-flow related mechanisms is therefore as follows:

$$p_{air-flow\ related}^2 = b \left( F_c^2 \Gamma^{-1.5} S^{-2} \right)^{\beta_1} B^{\alpha_2} U^4$$

### Cavity resonances

Inspecting measurement results one can observe that for low speeds and quiet road surfaces the levels in some third octave bands are rather high anyway. This is especially true for the 500 Hz band. While slick tyres do not show this special behaviour, patterned tyres do. For each speed and for a certain number of blocks per circumference the main excitation frequency created by the impact of individual tread blocks can be calculated. In the case of ca 50 km/h one obtains typically values between 450 and 500 Hz. At the same time in this range the second circumferential interior resonance in the cavity between tyre and rim takes place. Although the radiation of cavity resonances does not contribute significantly to the overall level at high speeds it can be an important mechanisms for low driving speeds. Therefore a model was designed taking into account the power spectrum  $G$  of the tread pattern variation

$$p_{cavity}^2 = cG_{pattern}^{\gamma_1}$$

The influence of the cavity contribution is visible in the figure below.

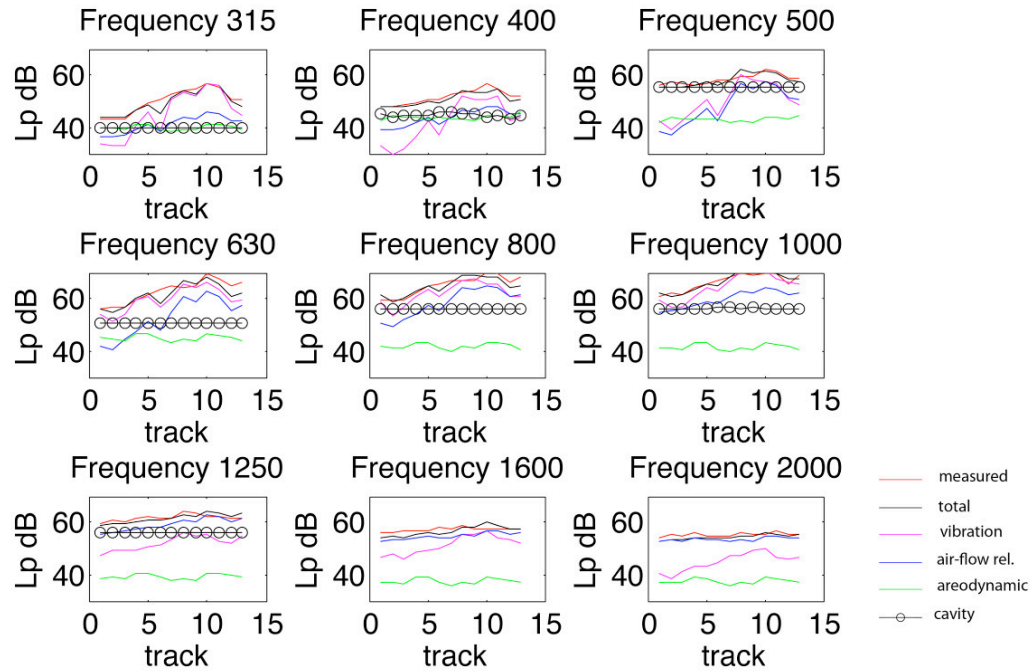


**Figure 12.** Contribution of the different source terms to the total calculated sound pressure in comparison to measured sound pressure levels at a speed range of 40 to 60 km/h. 14 different road surfaces, average over 4 tyres.

The figure shows the contribution of the different mechanisms to the total level as function of different road surfaces. While for most of the frequency bands the cavity resonances play a very small part (only for the very quiet surfaces track 1-3), this mechanism is dominant for almost all surfaces at 500 Hz.

### Aerodynamic vehicle noise

This part represents the aerodynamic noise from the vehicle itself and is based on measurements carried out in a wind tunnel for certain vehicles used in some of the mentioned measurements. This means that the coefficient  $d$  and the exponent  $\delta$  are given values.

$$p_{aerodynamic}^2 = dU^{\delta}$$

### Validation of the model

In the following it is shown with some examples, how well the statistical model may explain measured results. However, this may not always be the case (see the chapters Discussion and Conclusions). The following figure shows the difference between measurement and calculation for an average over 4 tyres.

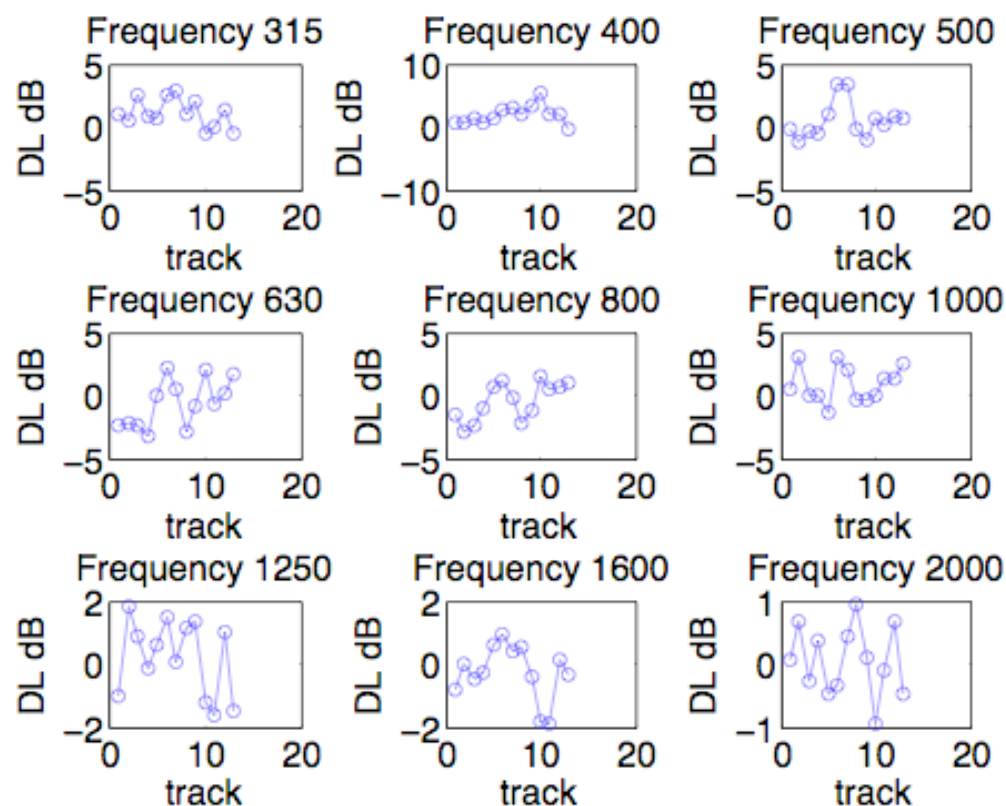


**Figure 13.** Difference between calculated and measured third octave band values (coast by) for the speed range 90 – 110 km/h as function of different road surfaces.

The differences are rather small apart from at lower frequencies where the measured and calculated values differ more. This might be due to the fact that results between individual tyres have a wider spread here, and that the average over only four tyres might not be sufficient. The comparison of the overall level is shown in the figure below and indicates that

there is a good agreement between measurements and predictions by the SPERoN model. The only bigger deviation is at surface 6 in the order of 2 dB.

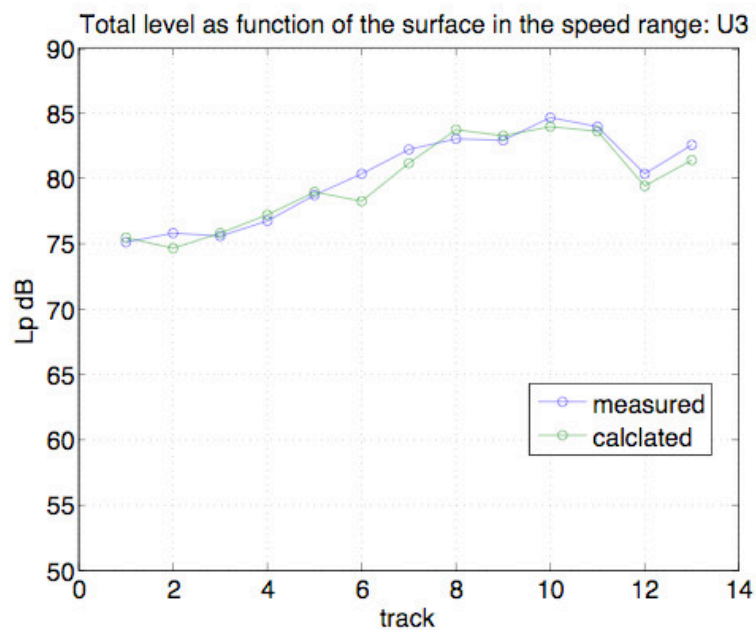


**Figure 14.** Overall levels predicted and measured for the coast-by situation as a function of the road surface at a speed range of 90 – 110 km/h.

### 3. Visual design

This chapter describes the different steps of the design procedure, which was focused on general and product design and meant to form visual concepts before moving on to acoustic design. The simulations, evaluation and pattern modifications (see figure 15) with focus on sound design are presented in chapter 4. The general workflow for the thesis is illustrated in the picture below.

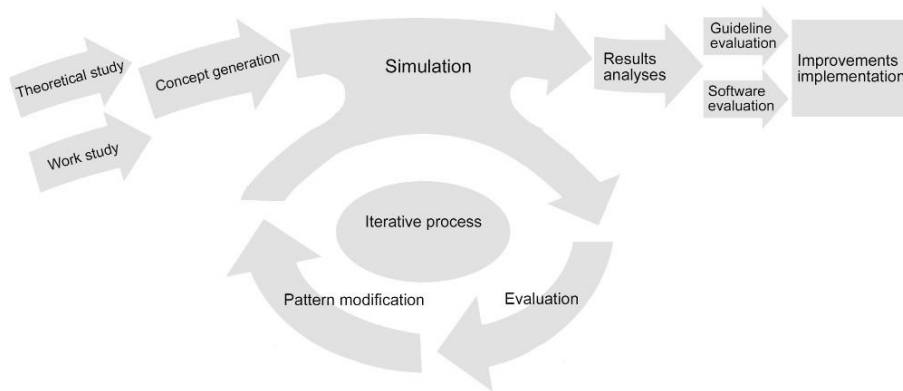


**Figure 15.** Workflow.

#### 3.1 Design Format Analyses

As in any company there are given traditions and methods for working that are not spelled out, but function in the environment from which they also originated. This natural structure sometimes makes it difficult for external observers to directly see where things come from. At first sight, designs of other Continental summer tyres, and especially those of the previous versions in the Continental Sport Contact series, seemed to be joined by visual similarities, as compared to other manufacturers' brands. In order to investigate this, a Design Format Analyses (appendix I) was made, involving tyres from six large companies providing similar products. The DFA showed that Continental in the past involved a large part of short straight grooves and clear and dominating circumferential grooves in their tread designs. The so called "Conti-rib", a thin circumferential rib that was originally there for stability, but later stayed purely for visual design purpose, seems to constitute a major part in this design tradition. It seemed a logical step to create new patterns that would keep part of these features, which appeared special for Continental style. From this viewpoint the concept patterns and expressions described below were formulated.

#### 3.2 Formulating guidelines at Continental

Much information about tread development can not be found in books or in any other type of literature. Part of the reason is that it is a narrow field, part of the reason is secrecy, tread design is one of the most secretive fields within the tyre industry. To gain an insight into possibilities and limitations of the development process one week was spent at the development departments for NVH (Noise and Vibration) and Styling (visual design) in Hannover, doing work studies and interviews. Seeing the development work under process and talking with people responsible for these areas was valuable for finding information about the whole process of tyre tread development, and about specific methods utilized in industry



today. Much information also came from phone interviews and email conversations with employees, during the thesis work.

The collected information was compiled into bullet points of helpful advice on how to design tread patterns with regards to several aspects. Emphasis was placed on favourable sound characteristics and information was also added from literature. These guidelines constituted the foundation for choosing pattern simulations.

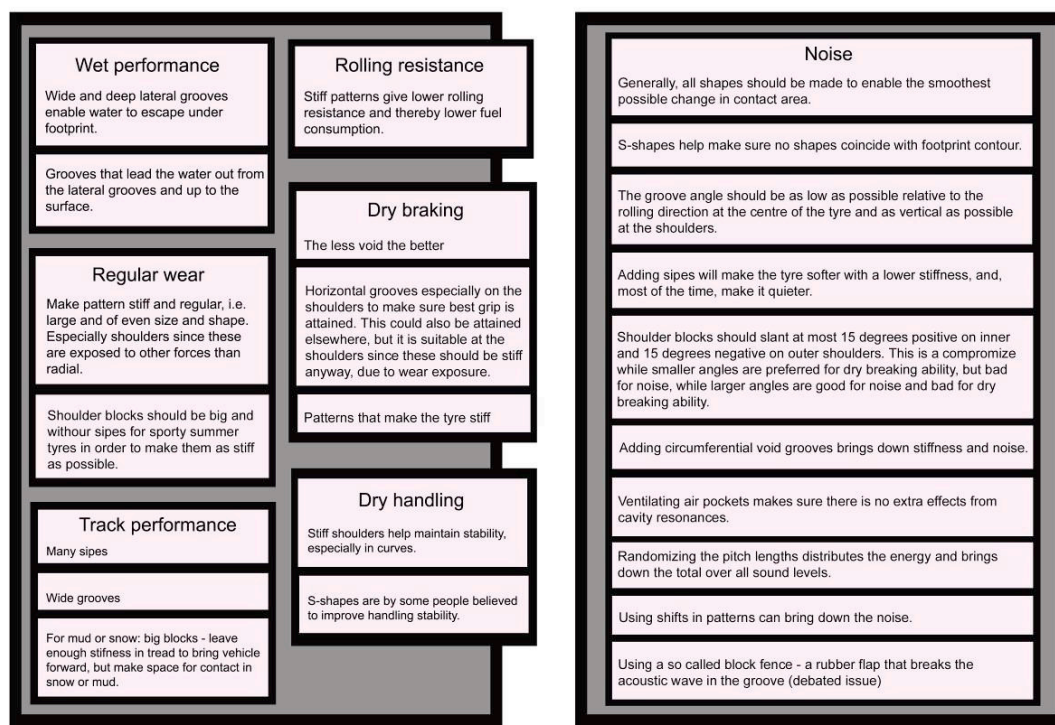


**Figure 16.** Guidelines

### 3.3 Functions matrix and product specification

Since this thesis focused on visual design, semantics should be an essential part of the product specification. The qualities that the product should express therefore first had to be found and explicitly formulated.

All products have semantic functions to express. Rune Monö [6] describes how a product even can express a quality that it has little or none of, just as well as it may own positive qualities without expressing them. It is therefore important to be aware of the possibilities for expressing the positive qualities inherent in the product. The very strong limitations to the tyre shape, material, colour and dimensions leaves nothing but its grooves and sipes to express its qualities.

Before the concept generation process could start, a functions matrix followed by the brief product specification (Appendix II), were erected. The semantics part of the product specification was then set aside to be developed further. A set of expressions were created which correspond to the three first functions below. (The fourth function was met by the use of DFA.) These four functions originate from Bühler's Organon model, which Monö [6] has described as the way in which signs convey functions between product and receiver. The first

function relates to cognitive ergonomics, how to understand how to use the product. For example, it may be requested for the pattern in the tyre to show the direction of rolling. This makes it easier to put it on, but is not important for driving the car. This function is often more essential for other products, where clues to its use are much more vital. The second function is important when selling the tyre, it should look as though it owns properties that the buyer wishes it to have (practical or not). Function three has more to do with appeal and with the buyer's emotional response to the product. The fourth function that talks about kinship was also answered by incorporating the results from the DFA into the concept generation.

1. *To describe*: purpose, mode of operation
2. *To express*: properties
3. *To exhort (appeal)*: reactions
4. *To identify*: a product, its origin, kinship, location, nature or category

### 3.4 Expressions and concept generation

To find the expression of the Continental brand for the new tyre tread designs, and to fit in the values for the customer, a values description and mood board were created. The mood board served as inspiration, and was also the basis for some of the expressions that were selected for the designs. Seven expressions, some of them newly created, were then the basis for sketching the patterns. Three of them represented Continental tyre as a brand and Continental as a company, while the other four represented the customer. Six patterns were then generated, partly from extracting ideas from the mood board, and partly on a combination of the expressions, of which one was a "Continental expression", and two were "customer expressions". By tying one expression in each concept to the Continental brand and company the three functions above were combined with the function *identify*.

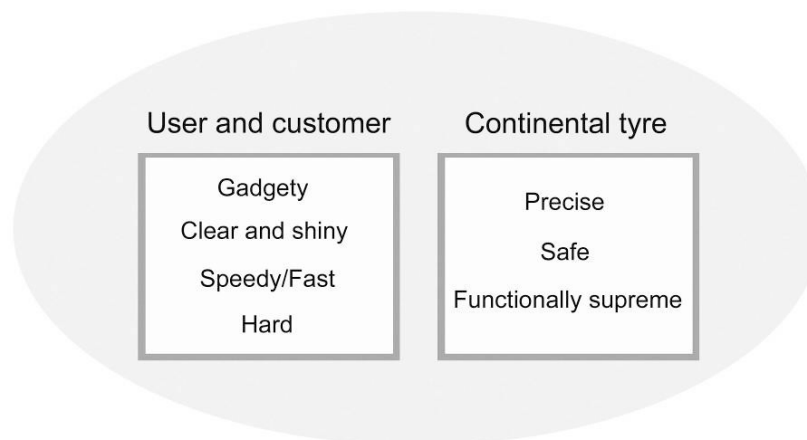


**Figure 17.** Customer and Continental words.



**Figure 18.** Mood board

### **3.5 Concept results**

Six concept patterns were generated that would fulfil the basic requirements in the product specification, which also included a basic manufacturing limitations such as repeatability, and also basic principles regarding solid mechanics (limiting the patterns to geometries that will not make the material too susceptible to mechanical damage). The patterns were drawn first by hand, then in Photoshop to enable a high flexibility of output formats. All patterns were drawn with grooves represented as black areas, while rubber that would have a chance of contact with the ground was made white.

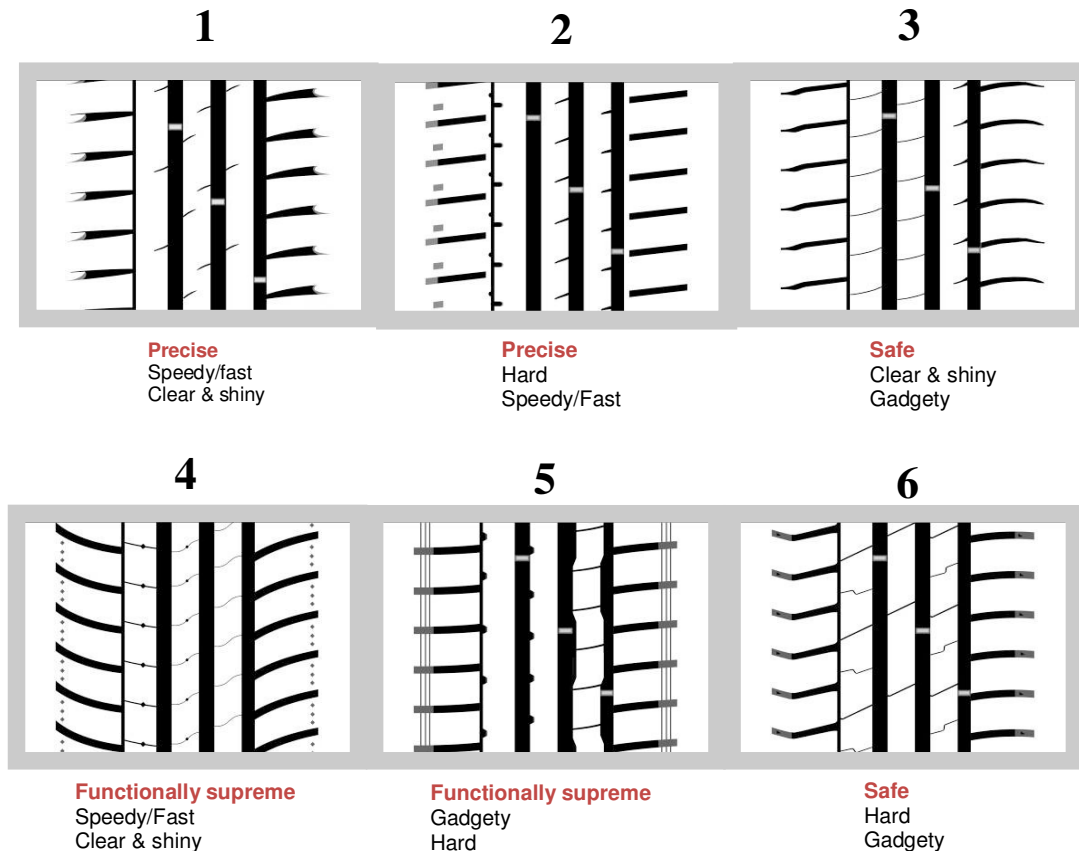


**Figure 19.** The six concept patterns.

### 3.6 Concept evaluation

After generating the concept patterns a short questionnaire was used to evaluate the expressions of the concepts. This particular survey was made only to receive a general indication about how 10 people, of various background, appreciated the six designs. The subjects were instructed that this is highly subjective and they could use their “gut feeling” and put anything they wanted, including comments on the sheet, but they also had to choose three of the available seven expressions, and only one from the user/buyer/customer box and two from the Continental box (figure 17). The survey showed that most of the designs according to this study were perceived to illustrate the expressions they were intended to illustrate. For results see Appendix IV.

## 4. Acoustic design

### 4.1 Pattern alteration procedure

After generating pictures in Photoshop these were made into bitmap files, transferred and processed with Matlab, from which the simulation software retrieves data. Material data and structural geometry data for another Continental tyre had already been prepared and installed from previous research on roads. To get started with the simulation process within the limited time of this thesis work this data was used. Each pattern had to be totally repetitive, without interruption due to misalignments between two repetitions. Any misalignments could cause a disrupted pattern when repeated, and would be likely to evoke larger vibrations that could lead to a higher total emitted sound level. The coarse adjustments to make repetitions smooth were therefore accounted for in Photoshop, while fine adjustments were made in Matlab. Simulations were then run in SPERoN at a constant velocity of 90 km/h, with constant inflation pressure and air flow resistance. The selected road surface was a surface called A141, which is very similar to a smooth ISO surface.

Patterns were then modified to investigate some already proven methods for improving sound characteristics. Some basic characteristics (which are also known to make a big difference in obtaining improved sound characteristics) were evaluated in these simulations, there among:

- Void content
- Shoulder groove angle
- Width of horizontal grooves
- Randomization
- Shift

By simulating, and hoping to confirm what was expected in terms of general tendencies resulting from these basic modifications, some of the concept patterns were meant to undergo modification towards a better result. Other modifications of various patterns were also made, some for investigation of the accuracy of the software, some for finding the difference between basic patterns, and for improvements of the previously generated initial patterns.

By modifying and simulating repeatedly the expected outcome was to see the general tendencies resulting from modifications of these basic characteristics (bullet points above) in tread patterns.

### 4.2 Controlled void content

The first round of simulations was made with the six concept patterns, which had not been checked for the void content. This since the first assumption was that some small differences in void content would not make a significant difference. It was then decided that alteration of some patterns was necessary to make sure the void content was not going to influence later simulation results. The new patterns were run in a Matlab program to calculate the amount of void, and passed when the void was at 28% with a maximum deviation of one percentage unit. The difference in sound emission from the old patterns was small but noticeable (table 1).

Pattern	Void before	Void after	Difference	dBA before	dBA after	Difference
1	28,73	28,30	-0,43	75,5	75,3	-0,2
2	28,50	28,04	-0,46	74,9	74,9	0
3	26,87	27,91	+1,04	74,9	75,1	0,2
4	29,95	27,83	-2,12	75,9	75,6	-0,3
5	30,14	27,71	-2,43	76,0	75,6	-0,3
6	29,18	28,04	-1,14	75,7	75,6	-0,1

**Table 1.** Void volume before and after modification and corresponding change in total A-weighted sound pressure level.

Modifications in the patterns, to obtain 28% void, were made only on the shoulder grooves in order to keep the circumferential grooves unchanged for all patterns. The shoulder grooves were simply made thinner/thicker, to make the part of horizontal void more equal between patterns (since the shoulder grooves in most patterns mainly extend horizontally). The patterns that had their total void volume decreased (all except pattern 3) saw a corresponding decrease in sound emission, while an increase was seen for pattern 3 which had its void increased. The positive effects that a smaller horizontal void volume had on sound emission - on this particular surface - were clear. The graphs show in third octave bands the over all sound pressure level as perceived when the car is passing by at 90 km/h on the selected road surface. The frequency span has been narrowed in the SPERoN software to include the most important area for human hearing.

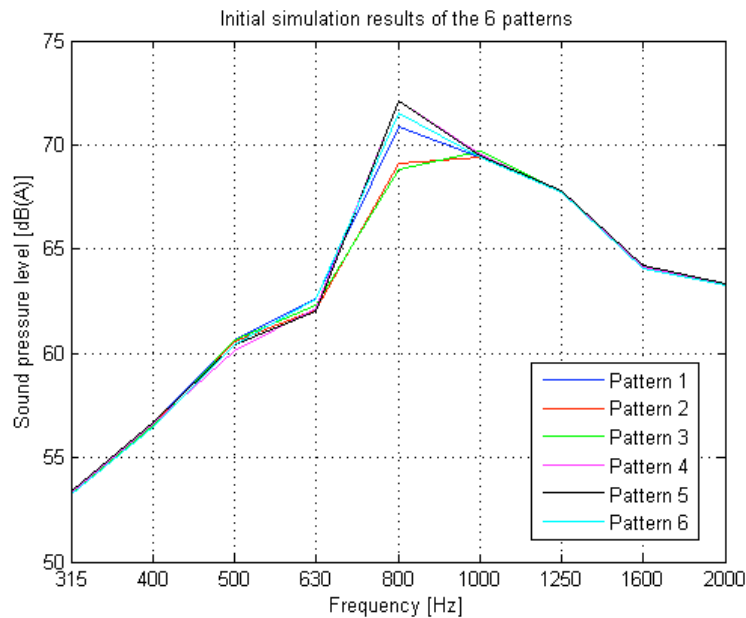


**Figure 20.** Six first patterns with different void volumes.

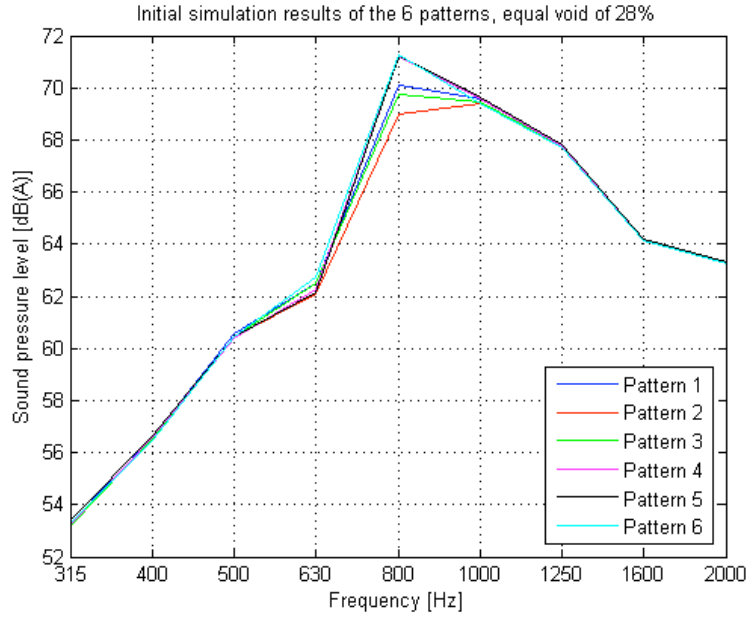


**Figure 21.** Six first patterns with void content adjusted to 28%. Note that patterns 4 and 5 are represented, but mostly hidden by each other and by pattern 6, since these differ so little.

In each of these six patterns the distance between each shoulder groove was 36 mm, which gave a total of 60 blocks per circumference. With this regular distance the main excitation frequency would fall at 694 Hz. However the main peak seems to fall at about 800 Hz. This is due to the construction of the tyre, which more than the tread pattern governs the excitation in this region.

The fact that each of the patterns were highly regular, and with clearly defined shoulder blocks, made the levels from the simulations quite high and the peaks clearer.

### 4.3 Larger angle of shoulder grooves

Pattern 2 was selected for the experiment with angle of shoulder grooves, since this pattern had shown better results than the others. The grooves on both shoulders were given an increased tilt of 5, 10, 15 and 20 degrees, relative to the horizontal line. No change was made in thickness of the grooves or of the total void content of the pattern. This way the circumferential void volume increased, while the horizontal void volume decreased. The results looked like expected, with decreasing levels for increasing tilt.

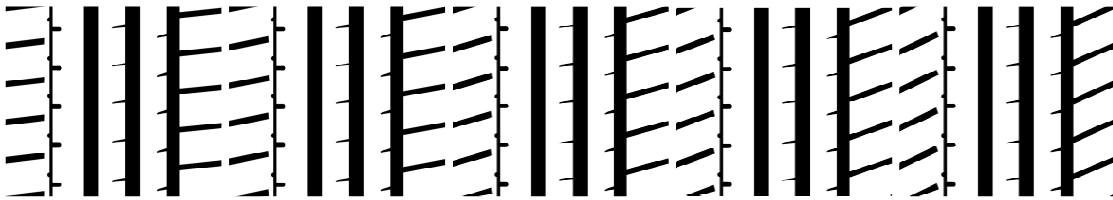


**Figure 22.** Pattern 2 with original angle (far left) of shoulder grooves and increasing angles (left to right) on both sides of the pattern, in steps of 5 degrees.

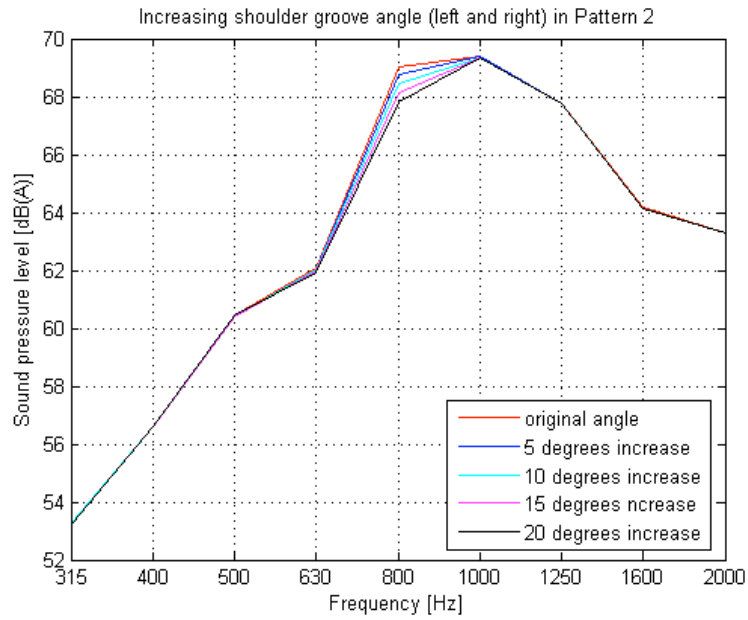


**Figure 22.** Pattern 2 with increasing shoulder groove angle.

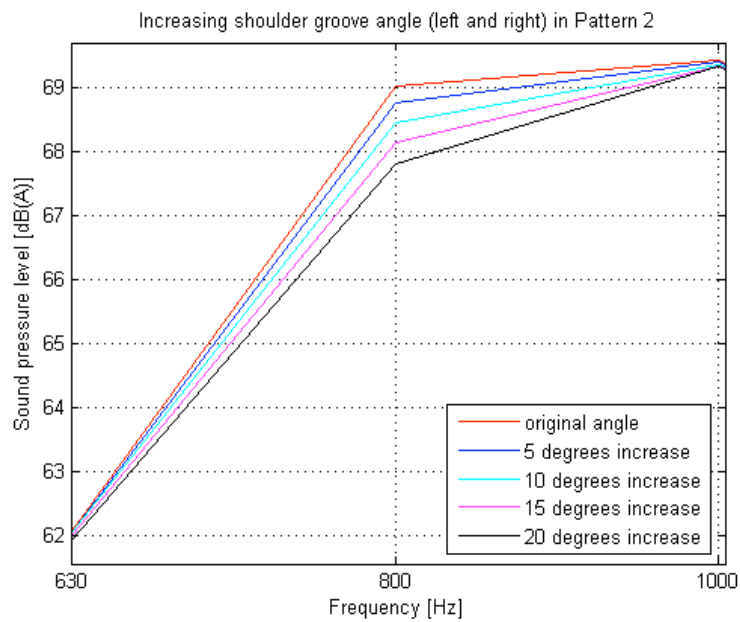


**Figure 23.** Figure 13 zoomed.

Pattern	[dBA]
Original angles	74,9
5° increase	74,8
10° increase	74,6
15° increase	74,6
20° increase	74,6

**Table 2.** Sound levels for increasing angles in pattern 2.



#### 4.4 Width of sipes

It was known that the resolution limit on the software may affect the results from simulations of patterns with small sipes, causing them not to show up in the simulation. Sampling was 750 bits per circumference, which meant  $2\,160\text{ mm} / 750\text{ bits} = \text{one bit every } 2,88\text{ mm}$ . With this sampling rate 1 mm thick sipes should only show up one third of the time, and give a misrepresentative value for the resulting sound levels. Pattern 1 was suspected to be particularly affected with a large number of sipes which were around 1 mm thick at the thickest place. With increased sipe thickness to 3 mm the chance of sampling in each sipe would be 100%. To see the influence of increased sipe thickness, Pattern 1 was modified to a sipe thickness of 3 mm, the void content of the new pattern was still within the set out range of 27,00-29,00%.

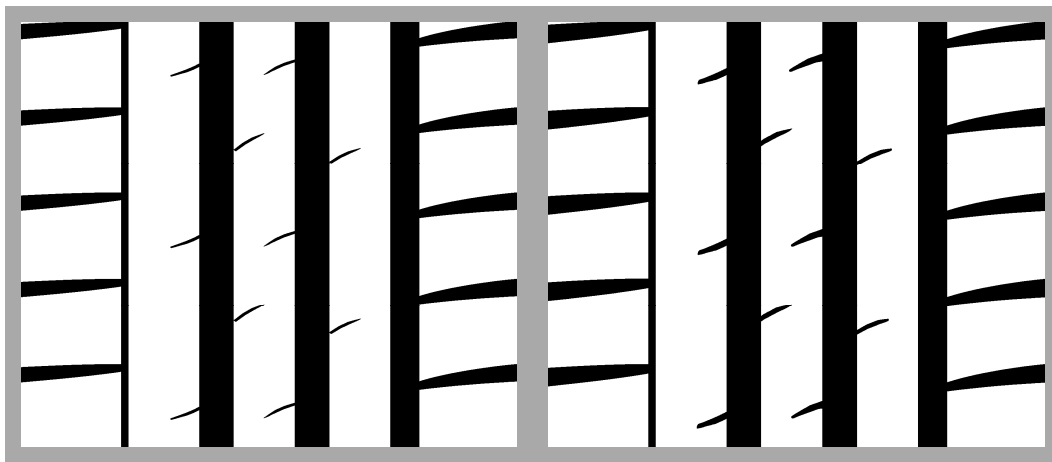


**Figure 24.** Pattern 1, with 1 mm (left) and 3 mm (right) thick sipes.

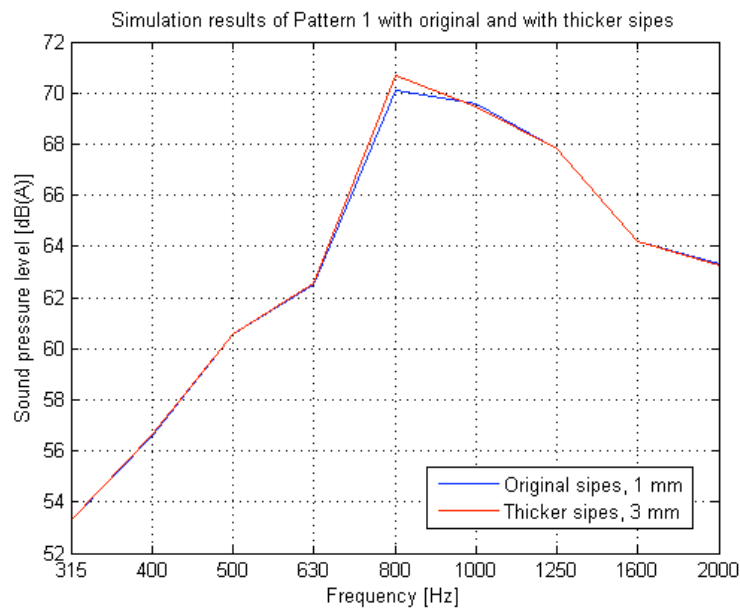


**Figure 25.** Results for pattern 1, with 1 mm and 3 mm thick sipes.

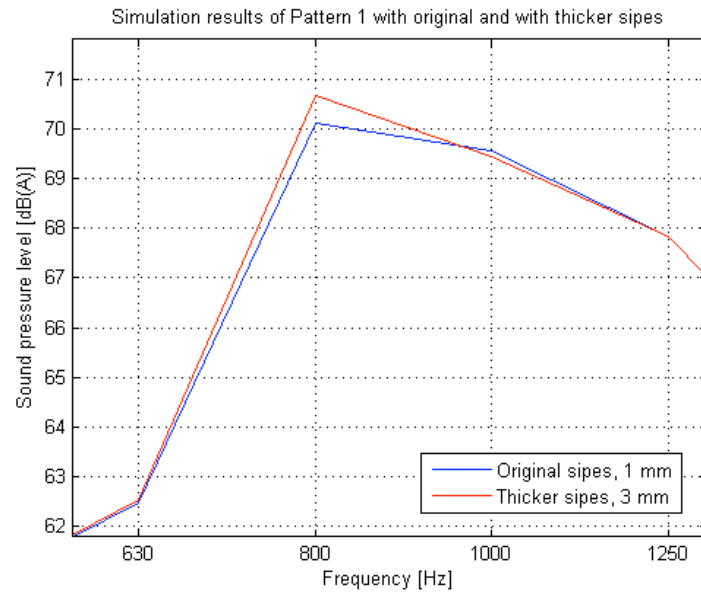


**Figure 26.** Zoomed view of Figure 30.

The difference in total level was also very small (table 3).

Pattern	[dBA]
original (1 mm)	75,3
Thicker (3 mm)	75,4

**Table 3.** Total dB(A) levels for patterns with different sipe thickness.

The sipes in pattern 1 had a strong horizontal layout and the result was therefore as expected with a small increase in levels, as the sipes were increased to 3 times their original thickness. It is also worth mentioning here that the decreased in stiffness which occurs when including many small sipes in the patterns is likely to lower the resulting sound levels. (This decreased stiffness may be taken into account, but was not for this thesis, by introducing a scaling factor in the program.)

#### 4.5 S-pattern simulations

Patterns based on S-shapes are frequently used in tread design. The shape in itself contributes to avoiding coincidence of grooves with the footprint. Therefore this was an interesting shape to investigate, even though the footprint in this software was square.

It is known that the width of a groove affects the sound emission, but exactly what the relation looks like is often unclear. It is also as highly dependant on the coarseness of the road surface. In order to view the difference between grooves of the same shape, but with dissimilar width, simple S-shaped patterns were constructed, each with a specific, constant groove width. Each pattern had the same outline, starting and finishing horizontally at the shoulders and crossing the centre of the tread with 30 degrees. Each S-groove had a constant groove width along its path and was identical to its neighbour. The circumferential lines were kept identical to that of the previous patterns. All patterns were tested for void volume, each fulfilling the previously set out requirement of  $28 \pm 1.00$  % void. Four patterns with groove widths of 3, 3.5, 9 and 17

mm were run in the simulations at 90 km/h. All other boundary conditions were held constant, as in the previous simulations. (The larger pictures are twice the length of the small ones to enable smooth repetition for the 9 mm pattern, and is compensated for when repeating in Matlab.)

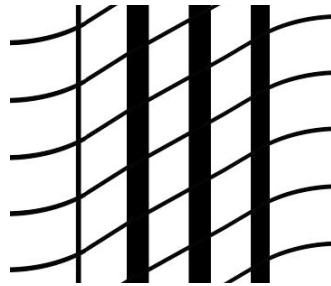


**Figure 27.** Grooves of 3 mm

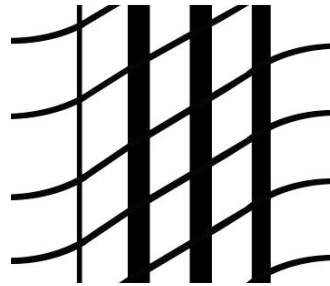


**Figure 28.** Grooves of 3,5 mm

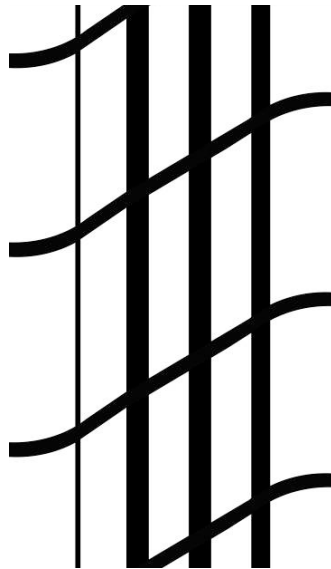


**Figure 29.** Grooves of 9 mm.

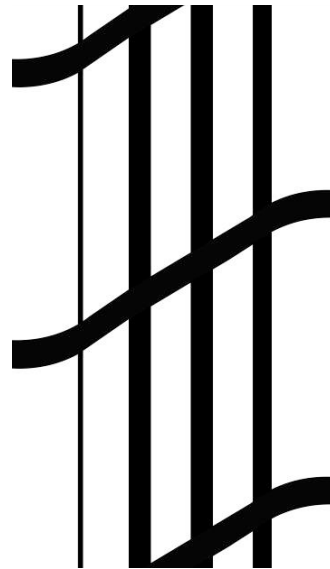


**Figure 30.** Grooves of 17 mm

Sandberg [2] describes the general influence of tread patterns on tyre noise. For cross bars (horizontally grooved patterns) an increase of groove width, if below 9 mm, will lead to an increased A-weighted sound pressure level. Above 12 mm width and increased groove width will lead to a decreased level. He further describes how an increase of angle relative to the horizontal line leads to a decreased over all A-weighted sound pressure level [1]. He does not describe similar limits for S-shaped patterns, but it was suspected that such patterns, with constant void and equal angles, would behave similarly to what he described for the horizontal patterns. S-shaped patterns with different width were therefore simulated with an expectation of similar results. The purpose of this was to look for tendencies that may help in choosing groove width for tyre patterns.

What is seen from the results of S-shapes is quite different from that described for cross bars above. The over all tendency is that the patterns with wider grooves give a higher level, regardless of how wide.

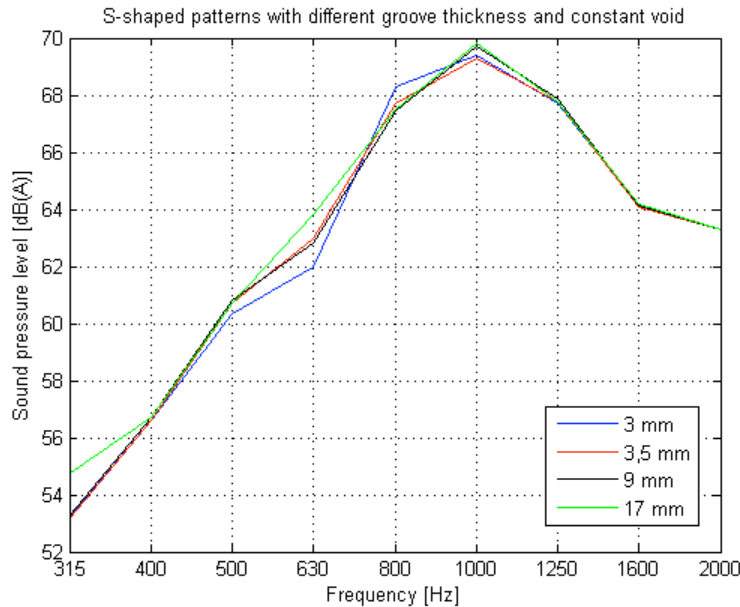


**Figure 31.** S-patterns, different thickness at 90 km/h.

What Sandberg writes about cross bars doesn't seem to be applicable to S-shaped patterns, at least not for constant void, or for the whole frequency range. In that case levels should instead have been higher for the two patterns with widest grooves. Instead the plot shows a varied behaviour between the four shapes. This is largely due to the fact that each pattern excites very differently to another. This should also be expected since each pattern has a different block length.

Frequencies that are dominant due to the repetitive nature of the blocks for these cases have been laid out in the table below for an easy overview. (This frequency is equal to the speed divided by the distance between each block repetition. The bracket shows the mid frequency of the 3<sup>rd</sup> octave frequency band to which the found frequency belongs.)

Pattern	Main excitation frequency at 90 km/h
<b>3 mm</b>	694 (630) Hz
<b>3,5 mm</b>	556 (500) Hz
<b>9 mm</b>	208 (-) Hz
<b>17 mm</b>	139 (-) Hz

**Table 4.** Frequencies that should be excited from the block sizes at 90 km/h. 3<sup>rd</sup> octave bands that the frequency belongs to are indicated by the middle frequency of this band in brackets. A dash indicates that the band is outside the current range.

The main peak in sound emission is found at around 800-1000 Hz for all tyre tread patterns, and largely unaffected by pattern design due to several amplification effects, there among the horn effect and the A-weighting. In the lower frequency bands material and mass properties of the tyre usually dominate, and in this region all four patterns show almost the same behaviour. Since these amplification and filter effects have a strong influence on the results the expected main excitation frequencies (table 4) can not easily be seen directly in the over all sound level

plot. However, if we extract the sound emission that is due to vibrations only we can more clearly see the direct influence of the main excitation in the plot. The influence of these vibrations is for all patterns especially high at 1000 Hz and in its proximity.

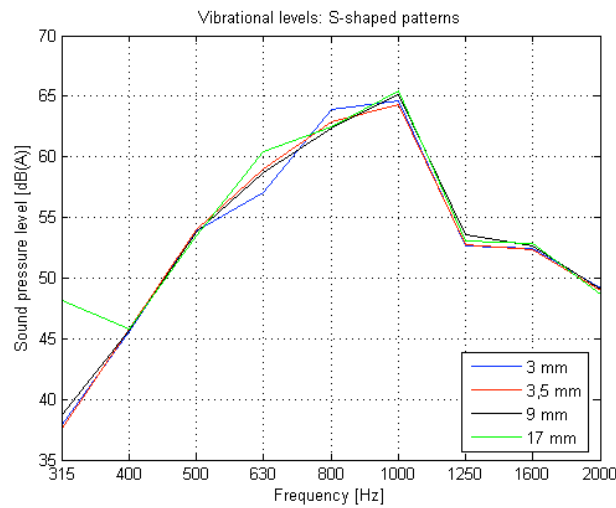


**Figure 32.** Sound pressure due to vibrations for the S-shaped patterns.

Even if some frequencies have very different results the total level is much the same due to the domination of the peak at 1 kHz (table 5).

Pattern/Velocity	90 km/h
3 mm	74.7 dB(A)
3,5 mm	74.6 dB(A)
9 mm	74.7 dB(A)
17 mm	74.8 dB(A)

**Table 5.** Total A-weighted sound level, for each of the S-shaped patterns.

#### 4.6 Basic patterns

The gathered general experience from interviews and from literature was that patterns with low void result in low sound levels on rough surfaces. Further a large part of circumferential void volume should be better than a large part of lateral void. Sandberg also states [1] that ventilating (linking) lateral grooves with circumferential grooves decreases the sound emission. With this background four patterns were tested: a blank pattern (no void), a pattern with only circumferential grooves, one with only horizontal grooves and one with both circumferential and horizontal grooves i.e. a checked pattern. All patterns apart from the blank had a void content of 28%. The tread with cross bars and the checked pattern were made with identical block lengths.

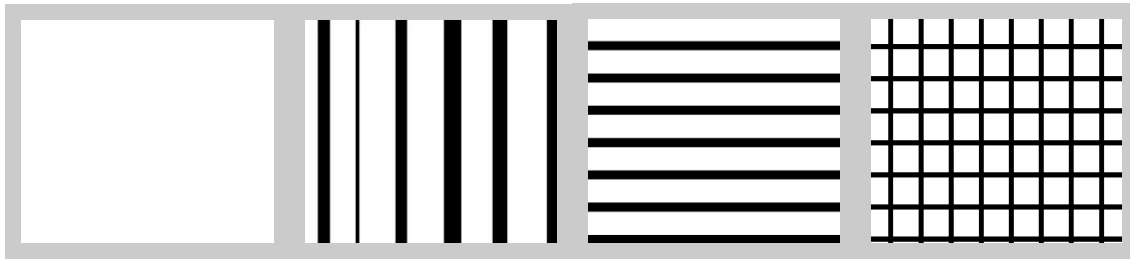


**Figure 33.** Slick tyre (blank pattern), circumferential grooves, cross bars (horizontal pattern), checked pattern.

Horizontal tread patterns are called cross bars. These are very much used in tyre testing and research, known to be most noisy of all patterns since they excite regularly in the driving direction. A tyre with a blank tread pattern is called a “slick tyre”. These are very quiet on totally smooth roads, but louder on rougher surfaces.

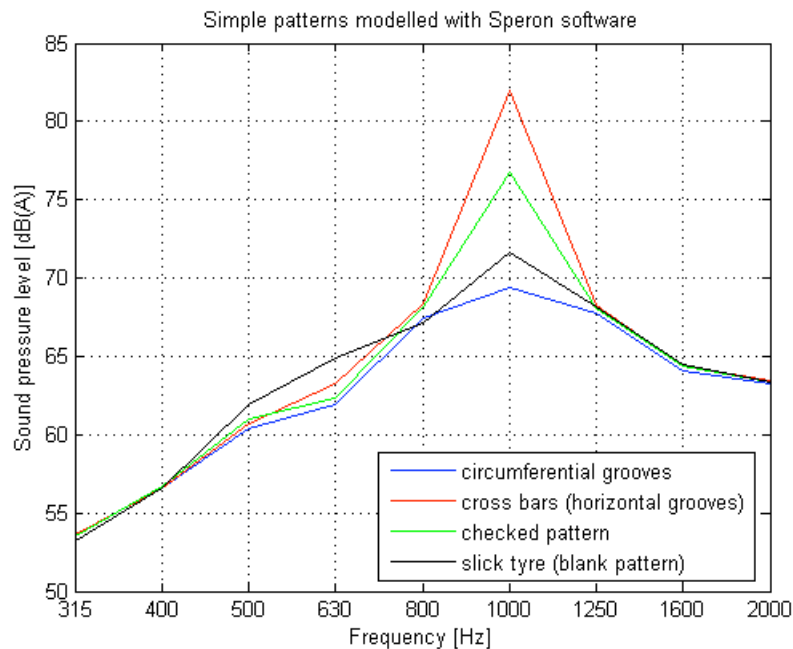


**Figure 34.** Simulation results for four basic shapes.

Basic patterns	[dBA]
circumferential	74,5
cross bars	82,6
checked	78,4
slick	75,7

**Table 6.** Total sound levels for the basic patterns.

The total levels for these patterns are just what can be expected from looking at the graph. The slick tyre radiates more than any of the others in the 500 and 630 Hz bands. The reason

for this is unclear, but it is clear it distributes the energy differently than the others. The pattern with only circumferential grooves has more circumferential void and doesn't either have any repetitions with shoulder blocks and is therefore quieter than all the others. The cross bars and checked patterns each have 84 repetitions per circumference. This means that these patterns excite strongly around 972 Hz at 90 km/h, which happens to be in the 1 kHz band. The 1 kHz band in its turn is highly favoured (amplified) by many mechanisms (as mentioned previously) and the peak therefore reaches over 82 dB(A). Since the main contributor to the over all levels as already mentioned is the part coming from vibrations, and this part rapidly falls above 1 kHz, this has a strong influence on the total sound level result.

A background to this explanation is found by looking at the stiffness curves of the four patterns. The x-axis shows the sampling points (750 points) per patch of pattern (in this case 180 mm).

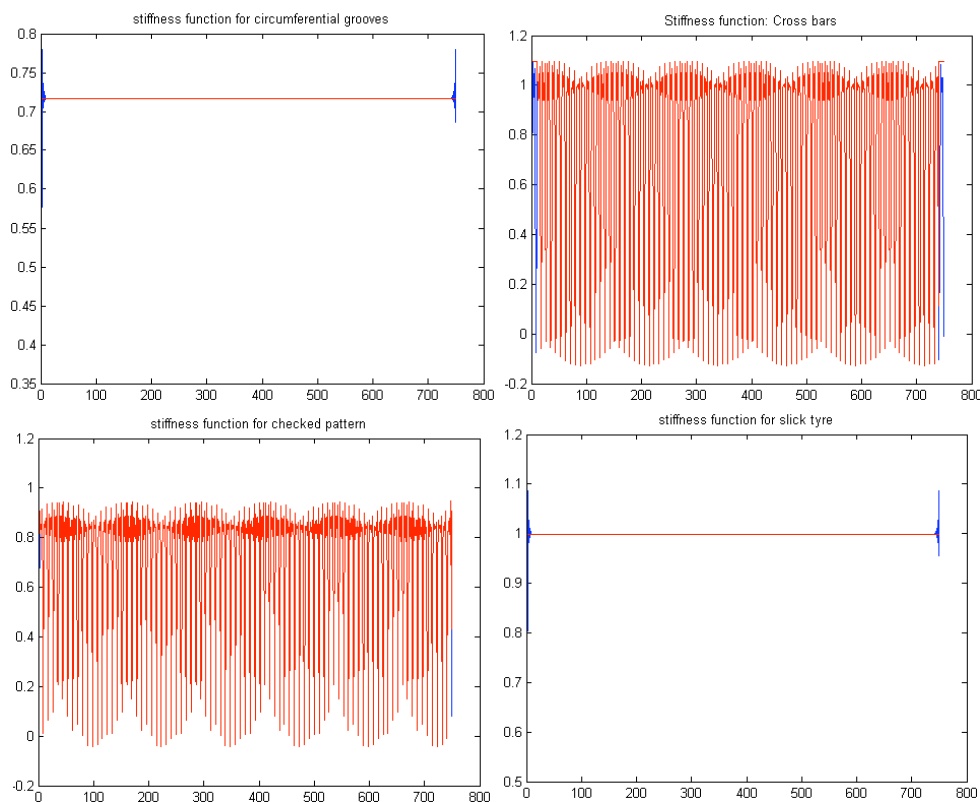


**Figure 35.** Stiffness functions for four basic patterns: circumferential grooves (top left), cross bars (top right), checked pattern (bottom left), and slick tyre (bottom right). The end values (blue in the graph) have been cut out whenever the deviation was very large, in order not to distort the simulation results. Instead graphs in red are what have been used as input for the simulations.

As expected, simulations showed the highest levels for the cross bars followed by the checked pattern and the slick tyre. The circumferential grooves gave the least emission. Its stiffness is relatively low since the void (28%) runs in the rolling direction, while the slick tyre has no void, which makes it very stiff, and therefore radiates more. (This is while it is run on a surface with some roughness, on an entirely smooth surface it would be quieter.)

It is not only the magnitude of stiffness that determines the sound generation, the dynamic range is also important. Looking at the stiffness range of the checked pattern explains why it

turned out noisier than the slick tyre. When the stiffness fluctuates like that the tyre will vibrate a lot and is more likely to cause sound generation.

#### 4.7 Randomization

Randomizing is very well used and is an efficient method for reducing the tonal components in the noise. The idea is to distribute the energy over a larger frequency spectra, which gives a flatter sound response curve. Usually three or four different pitch lengths are placed around the circumference of the tyre in an optimized sequence. Methods for finding the best sequences are refined and algorithms are involved along with other selective steps. For this thesis a hand made randomization was first made to pattern 1 to investigate the impact this could have on the sound level, then a series containing three pitch lengths, was created for the same pattern.

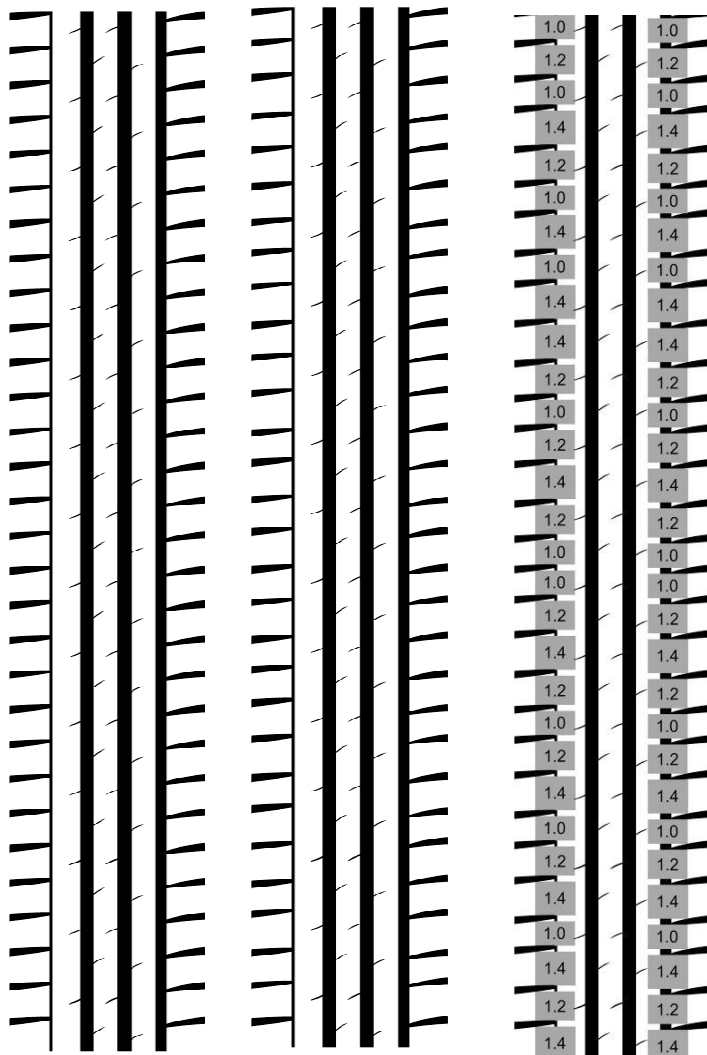


**Figure 36.** Pattern 1, totally even, no randomization (left)

**Figure 37.** Pattern 1, with totally random shoulder block size (middle)

**Figure 38.** Pattern 1, randomized with a sequence consisting of three pitch lengths (right)



The grooves in the first randomization were in both cases kept 6 mm wide as in the original pattern. In the first randomization the pitch length was varied, arbitrarily, as randomly as could be made with the eye (figure 26). The number of pitches in this pattern is therefore infinite. The variation of pitch is here very small, ranging from ca 0,8-1,2 of the pitch in the original pattern. To avoid accidental repetition of any internal sequence this pattern was made very long and repeated only twice in a circumference.

The second pattern (figure 27) used a pitch sequence containing three block lengths of 25, 30 and 35 mm (ratios of 0.83, 1 and 1.17). By letting the original pitch length be the middle sized pitch, letting the others constitute the lower and higher ratio, the number of pitches on the circumference was held constant. This was important to be able to compare at all with the original pattern. This sequence was also repeated twice in a circumference.

It should be noted that there is a vast difference between a randomized and an optimally randomized pattern. As seen below, these particular randomizations made the sound emission somewhat better, but a larger difference is likely to have been obtained had the pattern gone through the careful process of optimizing it.

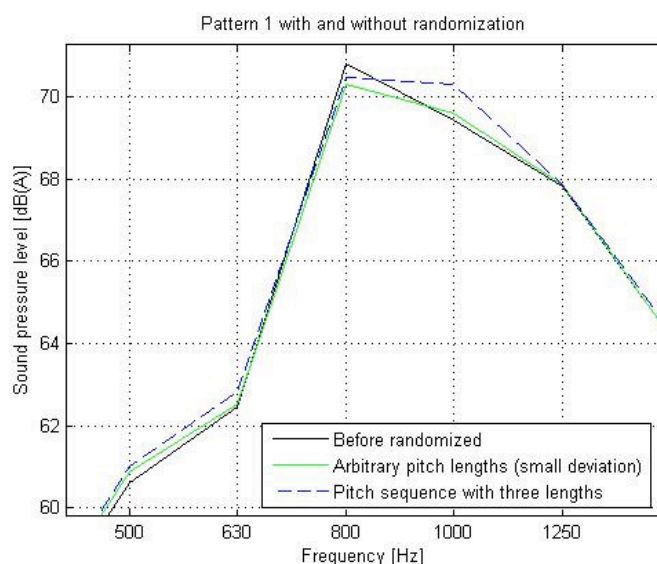


**Figure 39.** Results from the simulation. Over all sound levels. The patterns with randomized shoulder block lengths gave slightly improved results at 1 kHz.

The plot shows an improvement in the 800 Hz band, but a higher level in the 500, 600 and 1000 Hz bands. It is hard to say if the randomizations in this case may be considered successful. Sometimes the reduction in one band may be of greater importance than in another. However, the total sound level for the included spectra showed a small decrease from the original pattern on 75,48 dB(A) to 75,37 dB(A) for the arbitrary randomization. The randomization with pitch sequence reached the highest total level with 75,65 dB(A).

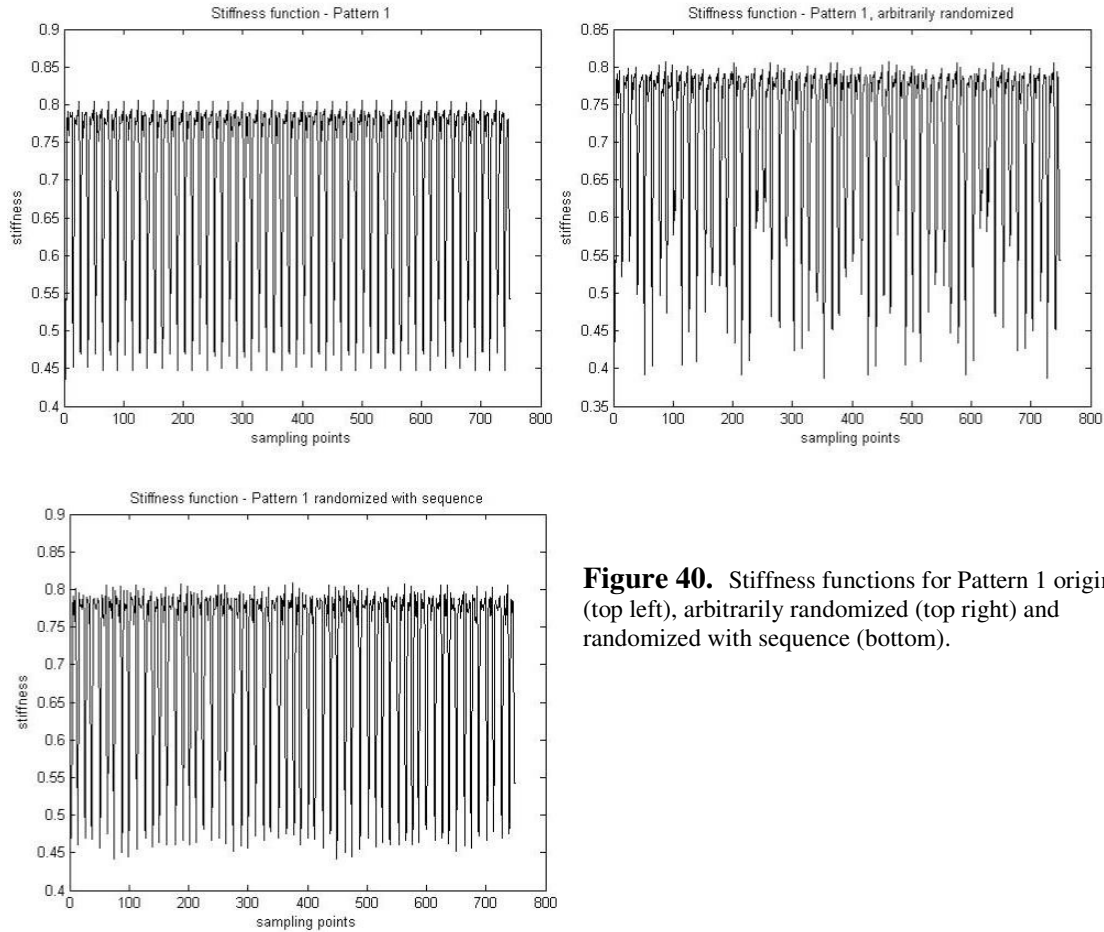


**Figure 40.** Stiffness functions for Pattern 1 original (top left), arbitrarily randomized (top right) and randomized with sequence (bottom).

Looking at the stiffness functions for these three patterns it is clear that they are very similar and that the simulated sound generation based on this would not be likely to show any large differences between the patterns.

#### 4.8 Cross bars with decreasing groove width but constant void and block repetition

There was a major problem in comparing the shapes patterns earlier, since the groove width was to be increased, but the void volume to be kept constant, in order not to influence the results due to changed void. The solution for this seemed to lie in increasing the block size (placing grooves further apart from each other), but as a result excitations arose in entirely different frequency regions and the patterns could not be compared with much gain.

To investigate the influence of groove thickness in a better way a cross bars, horizontal grooves, were used. Four patterns were constructed in which the grooves were given a thickness decreasing from 28 mm down to 8 mm, all with constant space between repetitions. Grooves were placed so that the distance between the block repetitions would be at the same constant distance between all four patterns, making sure that this time the main vibrational excitations would occur in the same frequency region for all of the patterns. This time decreasing shoulder groove thickness, while also keeping void volume constant was achieved

by compensating the length of the grooves, which were made to extend towards the centre of the tyre tread (figure 41).

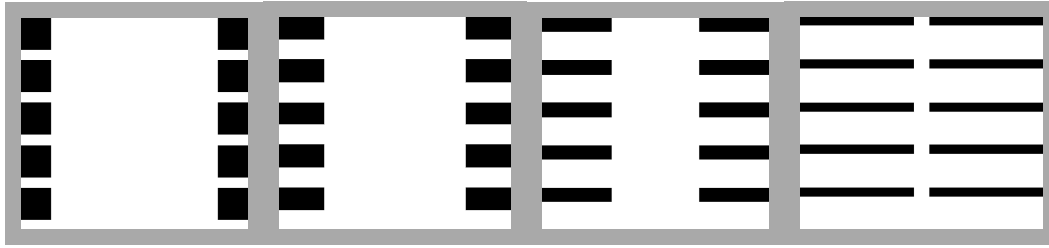


**Figure 41.** Patterns with constant void and even distance between each block repetition. Groove thickness 28, 20, 12 and 8 mm.

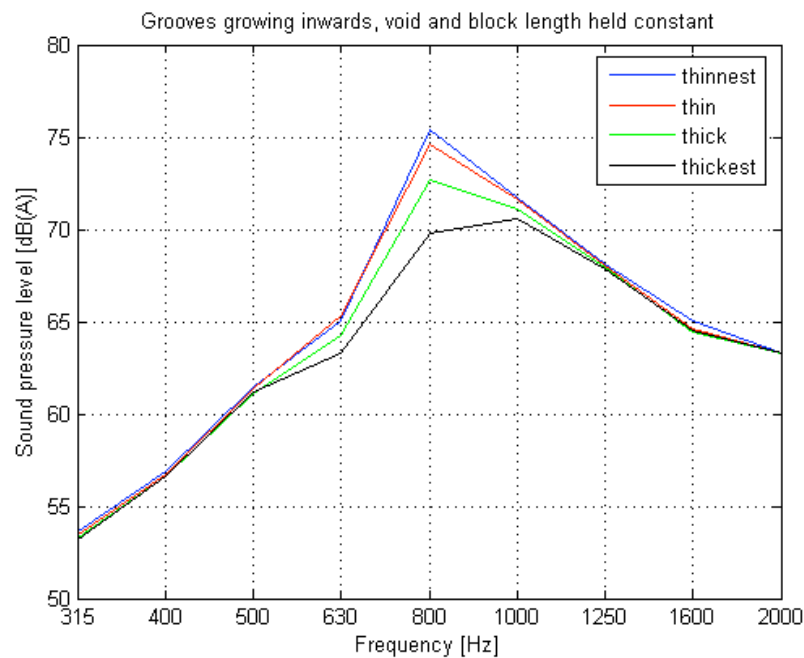


**Figure 42.** Results for patterns with decreasing groove thickness, but constant block repetition and void.

Groove thickness	dBA
28 mm	75,6
20 mm	78,2
12 mm	77,8
8 mm	78,2

**Table 7.** Total dB(A) levels for patterns with grooves extending inwards.

Looking at the stiffness functions a large difference is visible between the patterns, not in behaviour, but in dynamic range. The pattern with thickest grooves varies between 0,6 and 1, while the pattern with thinnest grooves fluctuates between nothing and all (0-1).

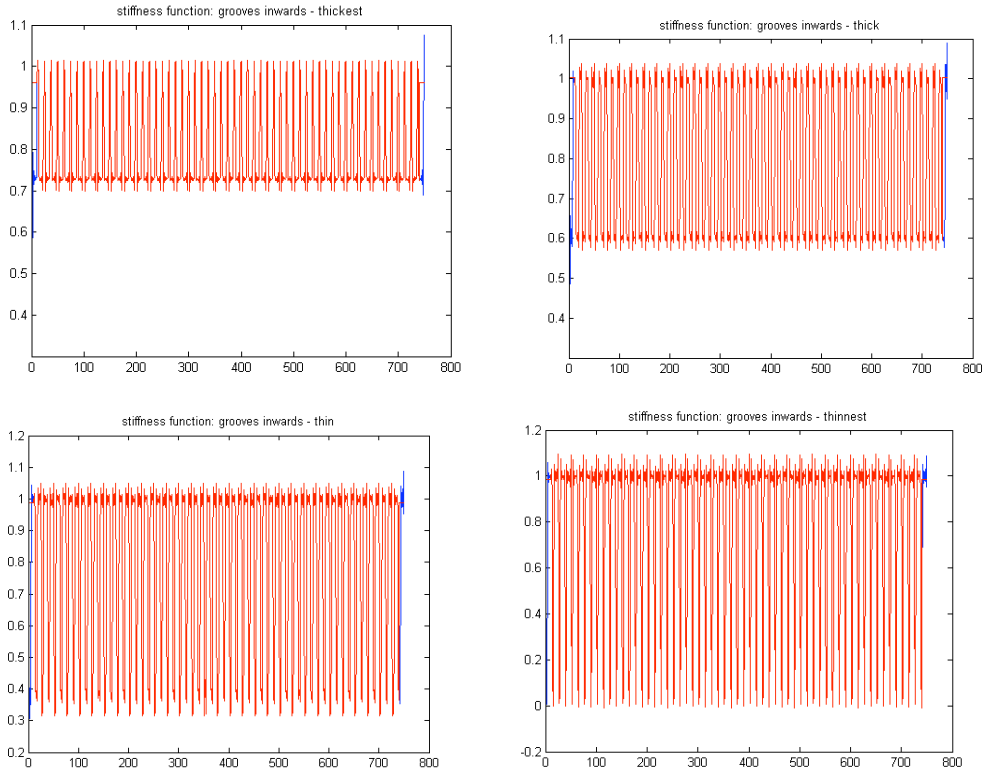


**Figure 43.** Stiffness functions for patterns with grooves moving towards centre.

The thickest grooves extend only slightly towards the middle. This pattern can therefore be likened with a slick tyre. The stiffness will therefore be relatively constant. When the grooves extend towards the middle it goes from resembling a slick tyre towards resembling a test tyre with cross bars, which are especially noisy. The dynamics of the stiffness increase. This is the sign of a large variation in contact force and is likely to cause a lot of sound generation.

#### 4.9 Shifts

The effect of shifts was also studied by running simulations of simple patterns with very large blocks and grooves. The blocks were shifted 5, 15, 20 and 30 mm. The groove thickness was made extremely thick with 30 mm in this case, and the block length was made equally large (36 blocks/circumference). This way a shift of 30 mm would imply that the groove on one side is countered by full contact with the ground on the other side.

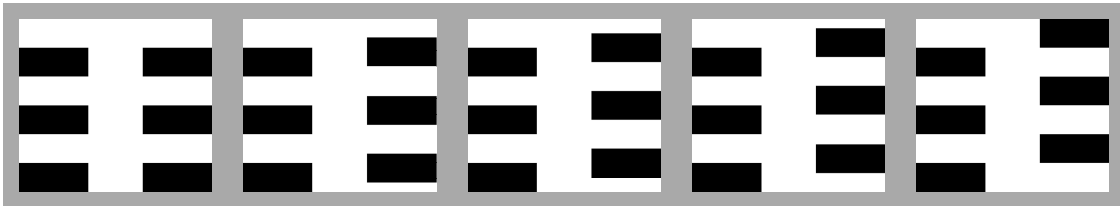


**Figure 44.** No shift, 10, 15, 20 and 30 mm shift.

Shifts	
No shift	77,3
10 mm	76,5
15 mm	75,9
20 mm	75,1
30 mm	74,1

**Table 8.** Total dB(A) sound levels for the shifted patterns.

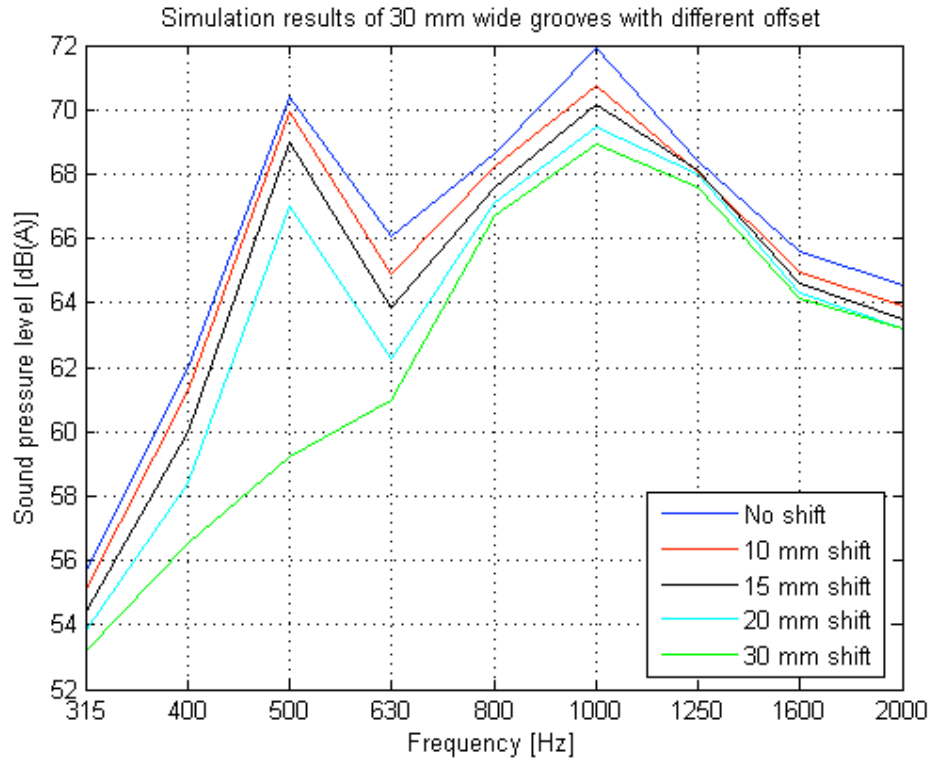


**Figure 45.** Results for the shifted patterns above.

Since the patterns have such a small number of blocks in one circumference the main excitation falls in a lower part of the frequency spectra than most of the previous patterns. The first peak is found at 500 Hz and its harmonic at 1 kHz, both very strong due to the extreme simplicity of the pattern.

Looking at the stiffness functions of these patterns we see that the pattern with no shift has the largest dynamic movement, and also the highest sound levels in simulation. Stiffness concentrations vary between around 0,3 and 1. The major impact of this stiffness, and the resulting high sound levels, is caused by the fact that large parts of void occur at the same time on both the right and left side of the tyre. Patterns with shifts have a smaller spread of stiffness concentration, e.g. for the 10 mm shifted pattern, whose stiffness has a focus at around the middle value 0,64. The reason this centre value is the same for all patterns is partly that their void is the same, and partly that the groove thicknesses too are identical. When the shift is 30 mm the stiffness will be very stable around 0,64 and the resulting low sound level is a direct result of this. In the case with 30 mm shift there will be full contact for 30 mm and then much less and constant contact for another 30 mm. This explains why the stiffness curve varies between 0,3 and 1 in all these cases.

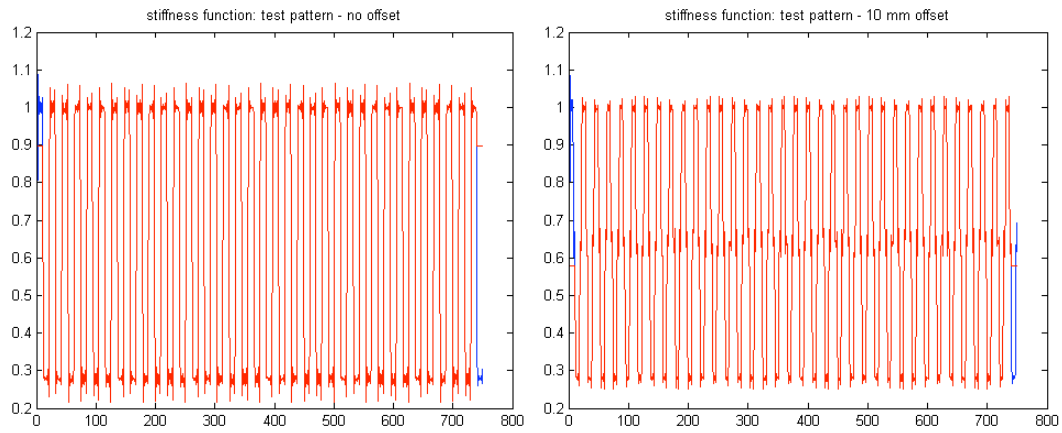


**Figure 46.** Stiffness functions for pattern with no shift (left) and with 10 mm shift (right).

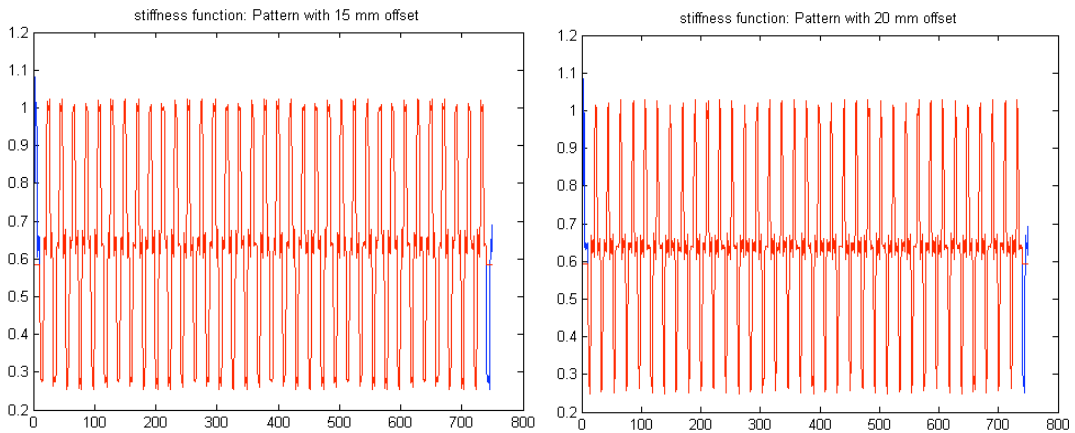


**Figure 47.** Stiffness functions for pattern with 15 mm shift (left) and 20 mm shift (right).

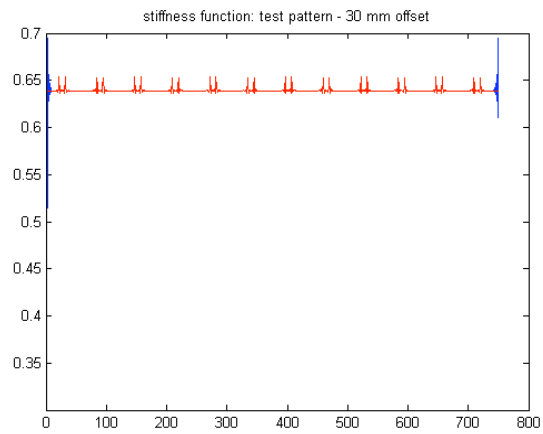


**Figure 48.** Stiffness function for pattern with 30 mm shift (shift equal to groove width).

#### 4.10 Shift on pattern 2

To round off the investigation of shifts, three different shifts were applied to one of the original patterns, Pattern 2.

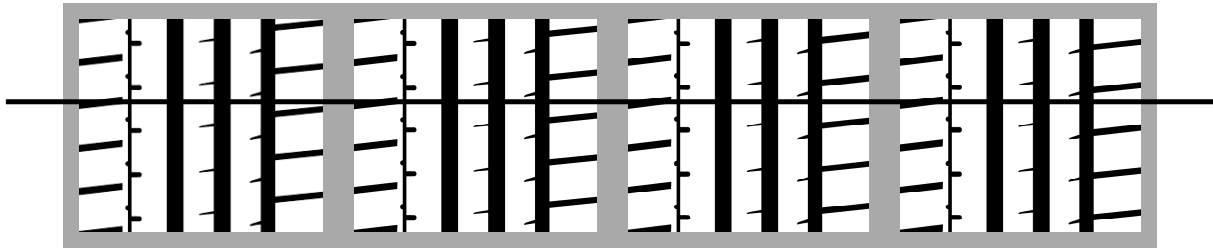


**Figure 49.** The initial Pattern 2 (left) and with the right shoulder shifted further down in steps of 5 mm.

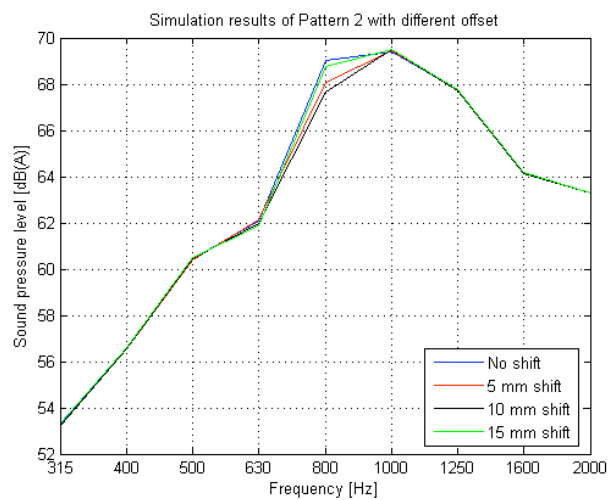


**Figure 50.** Pattern 2 with different shifts.

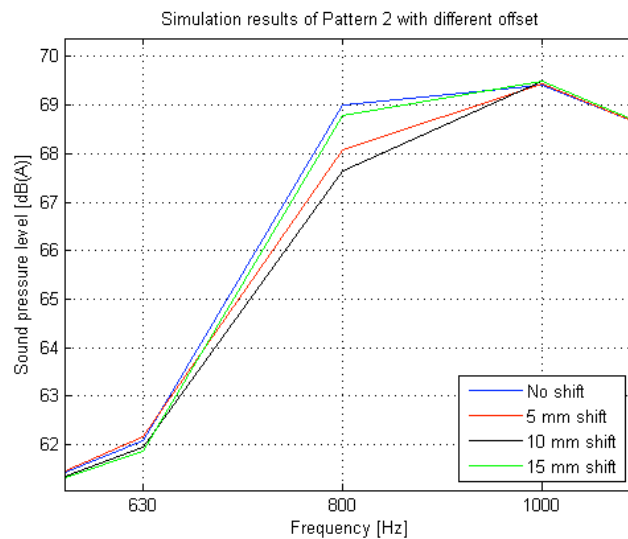


**Figure 51.** Zoomed view of Figure 41.

Shift on Pattern 2	[dBA]
Original (8 mm)	74,9
5 mm down (13 mm)	74,7
10 mm down (18 mm)	74,6
15 mm down (23 mm)	74,8

**Table 9.** Total levels for pattern 2 original, and with shifts introduced.

Results showed that the pattern could be improved about 1,5 dBA at around 1 kHz by introducing an extra shift of 10 mm to the whole right shoulder. The over all level was improved with 0,5 dBA. Pattern 2 already had a built-in shift. By now moving the grooves on the right shoulder down, creating more and more of a shift for each new pattern, the sound levels decreased for each of the new patterns, until the grooves reached the point where the shift started diminishing.

#### 4.11 Moving void

The SPERoN software is based on reading the amount of rubber available for contact, and from this and together with the other input tyre data for the structure, it calculates a hypothetical stiffness. Since this is the way the program is built weaknesses should reasonably include structural-mechanical behaviours. Even if the void volume were identical in two patterns, the geometry might not be. Therefore, it is also possible that neither is the stiffness of the structure, according to the rules of solid mechanics. In this test a small piece of void was moved to another location at the same height. With the void remaining at the same height the software would register the contact as identical for the two patterns, since void is calculated as a number of points on each horizontal line.

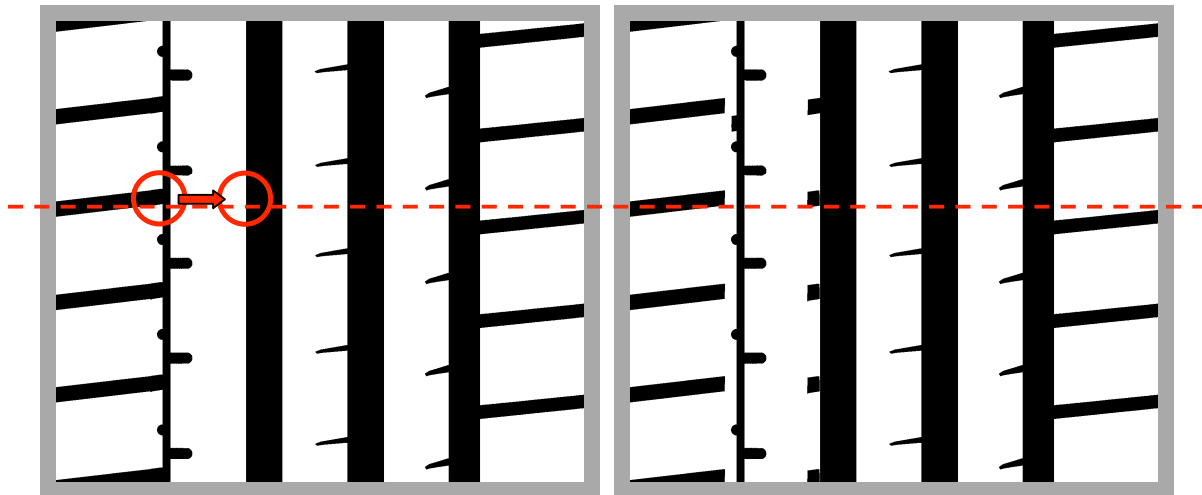


**Figure 52.** Pattern 2 modified. *Left:* Shoulder groove connected to the leftmost circumferential groove. *Right:* The void that was used to connect the grooves moved to a location on the same height, further to the right. The void has been moved to the right in the picture on the right, but stays in between the dashed lines.



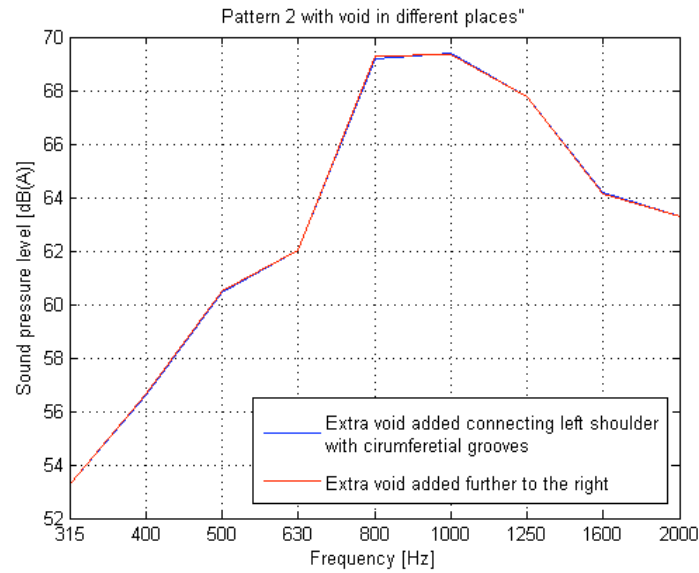


**Figure 53.** Pattern 2 in two cases: the shoulder groove connected to the circumferential line and the extra void in another position on the same height.

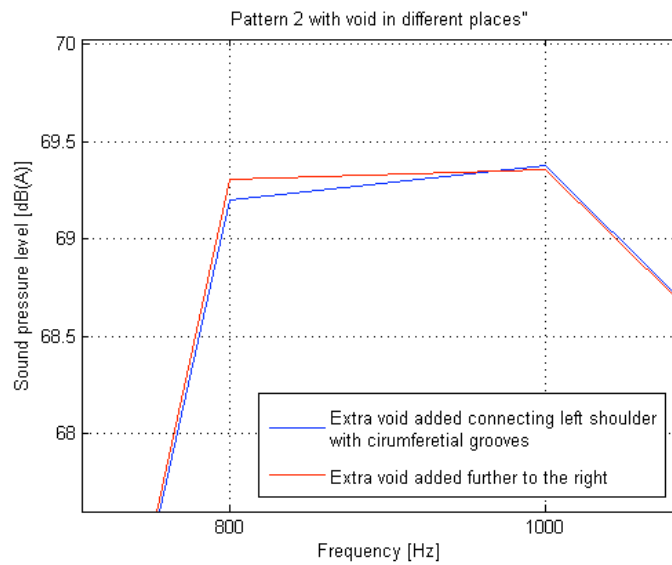


**Figure 54.** Zoomed view of Figure 53.

Moving void (Pattern 2)	[dBA]
Before	74,93
After	74,95

**Table 10.** Total levels for pattern 2 before and after moving the void.

#### 4.12 Improving Pattern 2 by combining methods

Finally, to investigate the outcome of multiple effects, shift, randomization and increased shoulder groove angle were all applied to pattern 2. It was hoped for, but not taken for granted, that the simultaneous use of the three methods would decrease the over all levels.

Pattern 2 was arranged with a series of different pitch lengths of 31, 36 and 41 mm (see figure 45). The shoulder groove angles were increased from ca 7 degrees (left) and 6 degrees (right) to 15 degrees in both cases. This angle was the maximum of what Continental would estimate to pass in dry braking ability (see guidelines). The shift that was found to be optimal in chapter 4.11 was used, which implied totally 15 mm (half the distance of the original shoulder block length) between the left and right shoulders.

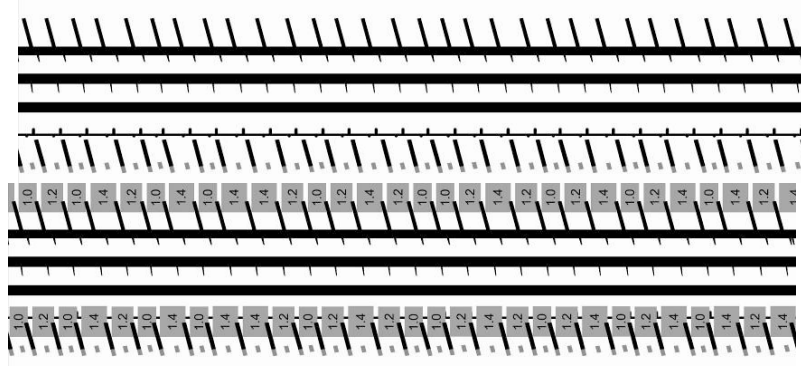


**Figure 55.** Randomized pattern 2 with shift and increased shoulder angles. The patterns in this figure are identical, but the lower pattern shows the used pitch series.

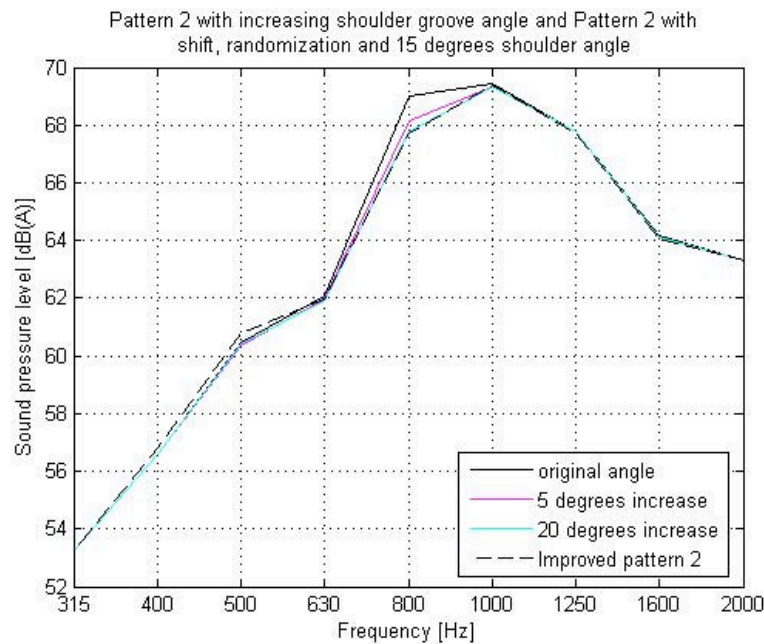


**Figure 56.** Results for pattern 2 with combined methods.

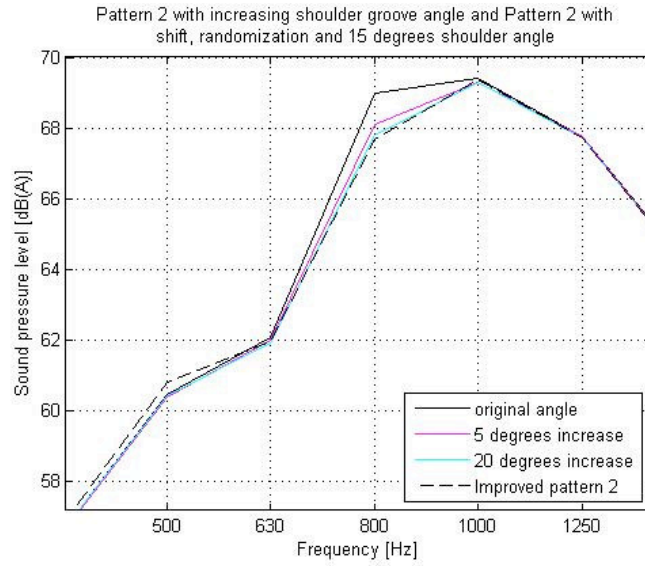


**Figure 57.** Zoomed view of figure 56.

Combined methods on Pattern 2	
Original 28% vv	74,9
Combined methods	74,6

**Table 11.** Total dB(A) levels for pattern 2 as originally , as with increased shoulder angle only, and with several methods applied.

Surprisingly the result showed very little improvement for the total level. This may be due to the complication of using several effects at once, e.g. the high angle may have required a different shift to work together, and vice versa, in order to give a less fluctuating stiffness. Further, the 1 kHz third octave band is slightly ungrateful due to its strong domination. Also the selected pattern was already good to begin with. It had some of shifts and angles built-in to start with. We also know from the simulations with randomization that the effects of this method can not be predicted unless it is combined with an optimization process. Nevertheless, a clear achievement was made in the 800 Hz band, where the combined methods gave an improved result of over 1 dB.

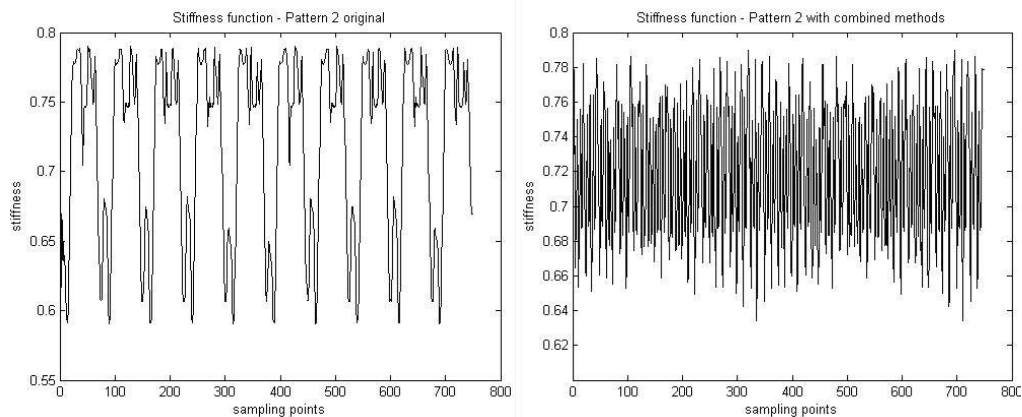


**Figure 58.** Stiffness functions of Pattern 2 original (left) and after the applied combined methods.

## 5. Discussion

As was seen in several simulations the magnitude and dynamic range of the stiffness function governed the sound emission in this software. It seems that keeping stiffness relatively constant and low might be a key to achieving quieter pattern designs. The important task is then to find the pattern which gives such a stiffness function. It seemed from the simulations and from the contact curves of several patterns, especially those with shifts (see chapter 4.9) and S-shapes (see chapter 4.10), that these promote keeping the total horizontal contact area more constant and therefore gave a low sound level. If one part of the tread leaves ground another should immediately take over for the best stiffness distribution and low sound levels. While this may lower the sound generation, this shift of contact back and forth sideways may affect such qualities as e.g. wet and dry handling very negatively, which also has to be considered. Apart from this it seems logical that the S-shapes, that are already popular in the tyre industry, are especially well suited since these enable very smooth contact changes and naturally involve shifts. They also give the designer large freedom in varying the shifts. For smooth repetition of a pattern over the circumference, however, these patterns have to be rather small not to become unaccommodating for repetition.

The fact that SPERoN does not take into consideration structural changes from alterations in geometry means that the softness, and therefore the real stiffness, can not truly be accounted for. Further software developments of the software would improve the accuracy. Knowing that the software does not take into account the softening of the material that occurs when geometry is changed, it can be expected that results should show lower levels from an increased sipe width. SPERoN should therefore not be used for evaluations that require accurate representation or are highly dependant on accurate mechanical descriptions of how the material's properties vary with different geometrical shapes. SPERoN will therefore be faulty if the bending stiffness is of major importance and is mainly influenced by the tread.

The resolution was intended for the original use of the software - for investigations of road surfaces. If it is to be used in more extensive simulation for tyre evaluation, resolution can beneficially be increased.

The idea of using a sequence in randomizations was to use a method similar to that which is used in industry today. However, the results are expectedly to be vastly different without optimization of the sequence.

The simulated patterns are all representative for one speed only, 90 km/h. Having looked at the other speeds it is known that this may well give quite different results. However, the choice was made to look at 90 km/h since this is a commonly used velocity that causes large environmental problems in the vicinity of main roads. The SPERoN software also provides the opportunity to sweep velocities in any interval between 0-100km/h.

## 6. Conclusions

SPERoN as a software shows high accessibility. Whichever stage in the process the product development has reached it works well for utilization and evaluation of the tread design. At anytime a sketch or drawing can instantly be simulated.

A strong limitation is that it does not take into account the smallest grooves.

The accuracy of input material data may also be questioned, since all rubber compounds and structures for are difficult to estimate. Especially for the target tyre for this thesis these data are somewhat different.

Offset and randomization showed to be great tools for decreasing sound emission, especially shifts. The simulations also confirmed that trading horizontal void for circumferential void (e.g. by increasing the angle of grooves) is a useful method.

From part 4.9, where grooves growing inwards were tested, it might be concluded that it is better to design large distances of no contact, i.e. a lot of vertical void, in the circumferential direction and have plenty of contact with the ground next to it, than to use thinner grooves and instead spread these across the tyre width, i.e. a lot of horizontal void. This information came out through the work as early as formulating the guidelines. In the guidelines this is partly represented through the guide stating that adding circumferential grooves to the pattern might be useful.

Designing for smaller dynamics in stiffness seems to be a solution to bringing down the levels. Two efficient methods for keeping the stiffness dynamics down were to introduce shifts and to increase groove angles relative the horizontal direction.

Designs that can be perceived as describing similar expressions may still give rise to very different sound generation. Pattern 2 and Pattern 6 were perceived quite similarly visually, but still showed very different results from the sound generation simulations. Pattern 2 was perceived as one of the hardest by most people, but was still the “softest” (quietest) of all patterns in the sound level simulations.

There is a limit as to when the impression of a pattern is altered or disrupted, (investigating this limit is outside the scope of this thesis). This limit naturally varies with the individual, and depends on the force in the rules of gestalt perception within the structure. The limit of disruption can be postponed if randomization and shifts are already a natural part of the pattern itself. This is the case in for example patterns that from a distance appear like an S-shape. The shift is inherent in the structure. Another way of inhibiting the occurrence of disruption is to compose the pattern with very strong perceptual interconnections, i.e. composing closely according to the rules of gestalt perception (See Monö 1997 for further reference).

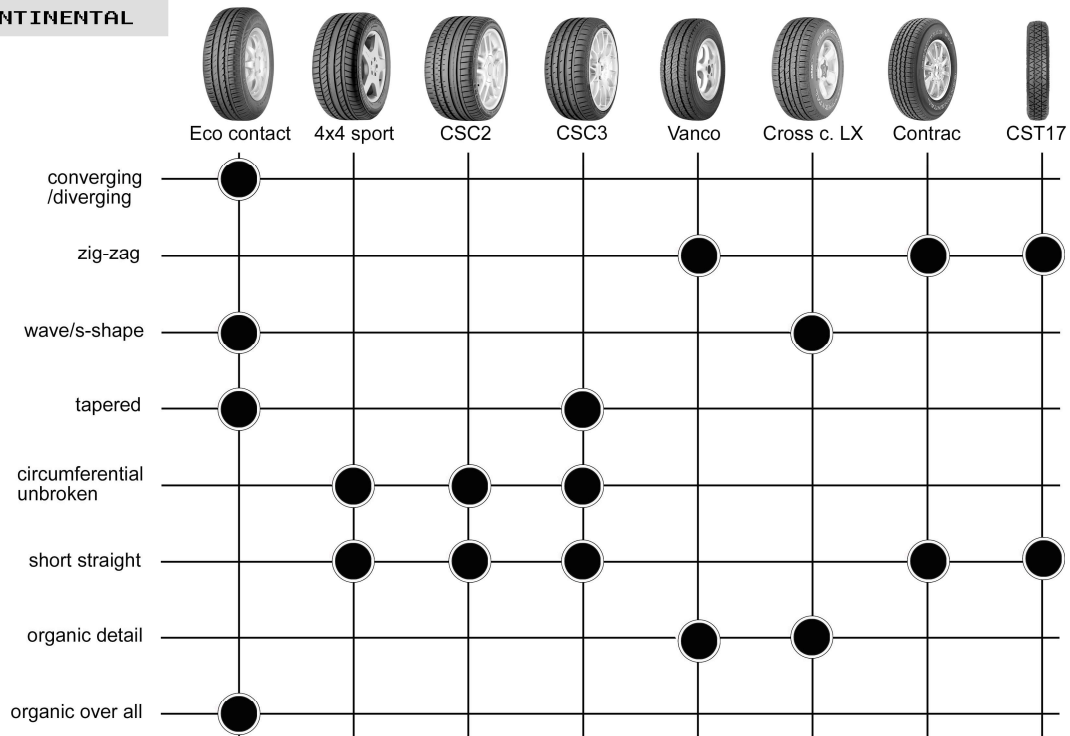


## 7. References

- [1] Sandberg, U. and Ejsmont, J.A. *Tyre/road noise reference book*. 2004. p 230
- [2] Sandberg, U. and Ejsmont J.A. *Tyre/road noise reference book*. 2004. chapter 7
- [3] *The tyre - rolling resistance and the fuel savings*. Michelin publications. Société de Technologie Michelin, 2003.
- [9] Kropp W., Structure - borne Sound on a Smooth Tyre, Applied Acoustics, 1989, Vol 26, p 181-192
- [4] Interviews with styling department at Continental
- [5] Interviews with NVH group at Continental
- [6] Monö, R. *Design for Product Understanding*, Rune Monö and Liber AB, 1997.
- [7] Johannesson, Persson, Pettersson, *Produktutveckling- effektiva metoder för konstruktion och design*, Liber AB, 2004
- [8] Collin, R. 2007-10-27, *Däcken som är dubbelt så bra*.  
<http://www.aftonbladet.se/bil/article971291.ab>
- [10] Kropp W., Structure - borne Sound on a Smooth Tyre, Applied Acoustics, 1989, Vol 26, p 181-192

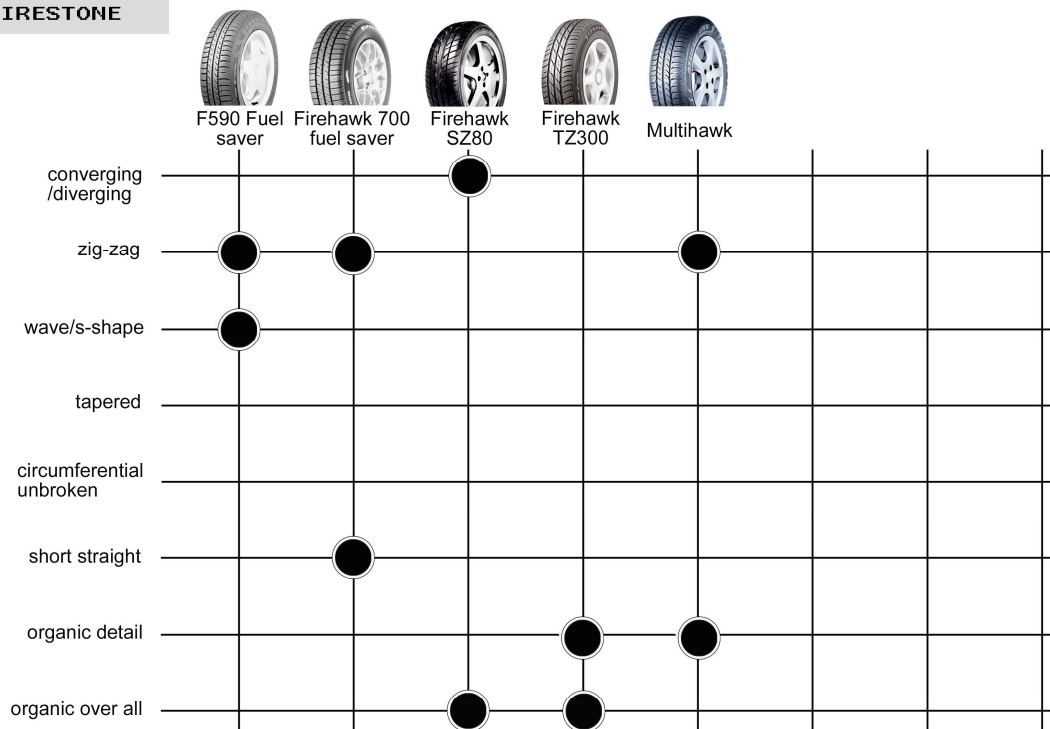
## Appendix I – DFA

### CONTINENTAL



Continental - Firestone - Hankook - Michelin - Nokian - Pirelli

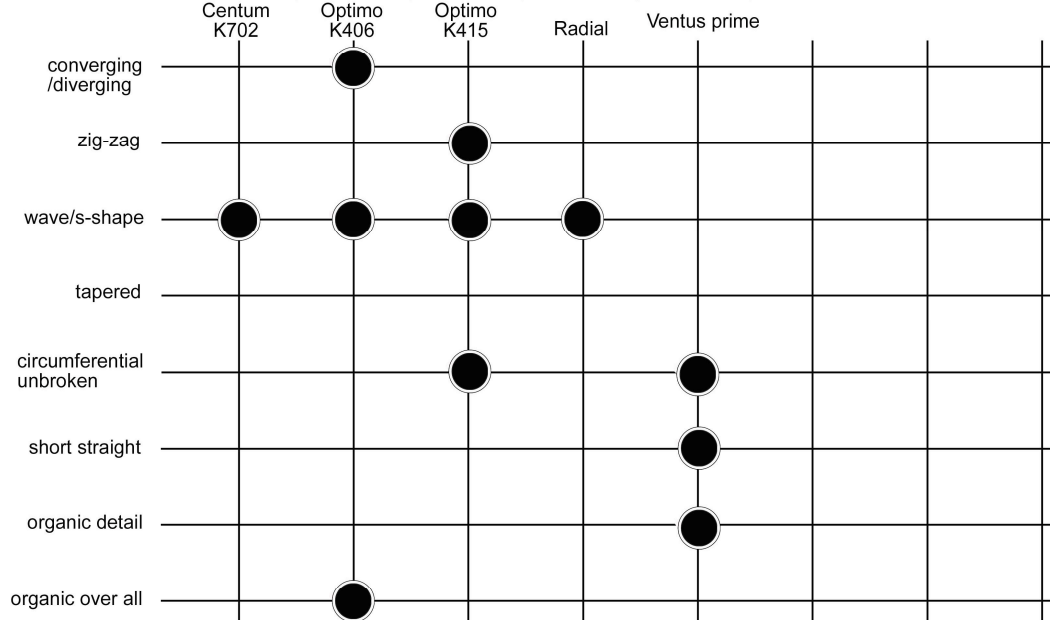
### FIRESTONE



Continental - Firestone - Hankook - Michelin - Nokian - Pirelli

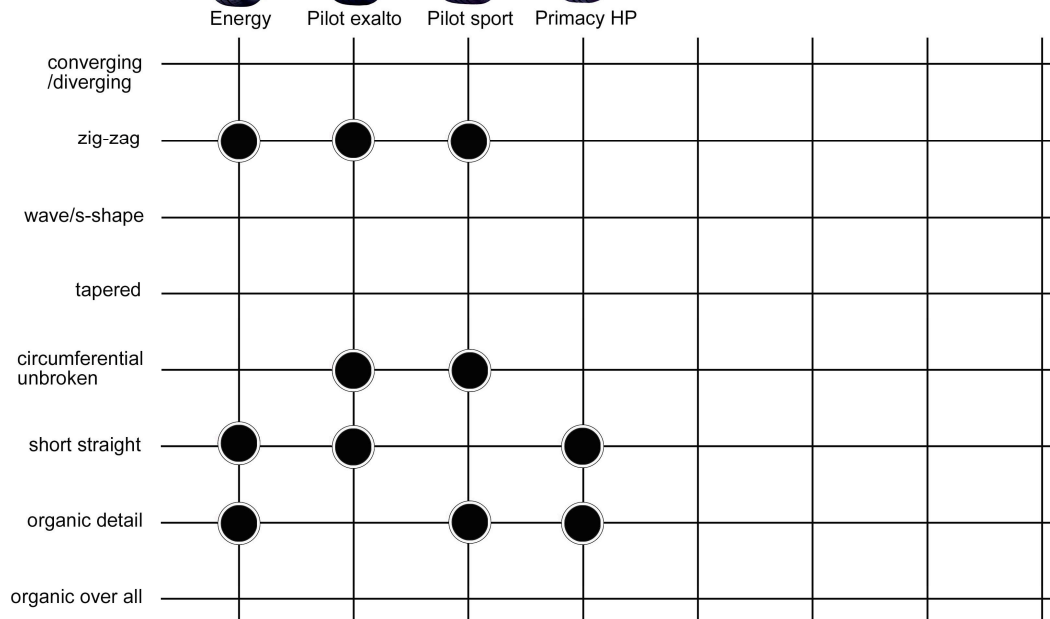


## HANKOOK



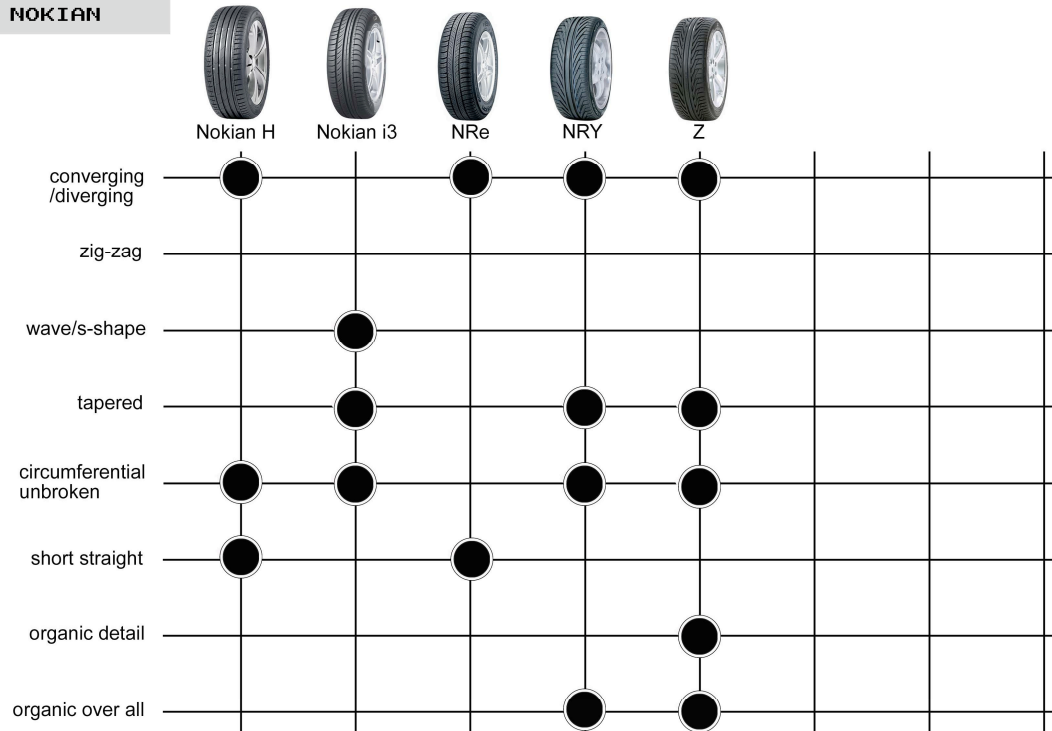
Continental - Firestone - Hankook - Michelin - Nokian - Pirelli

## MICHELIN



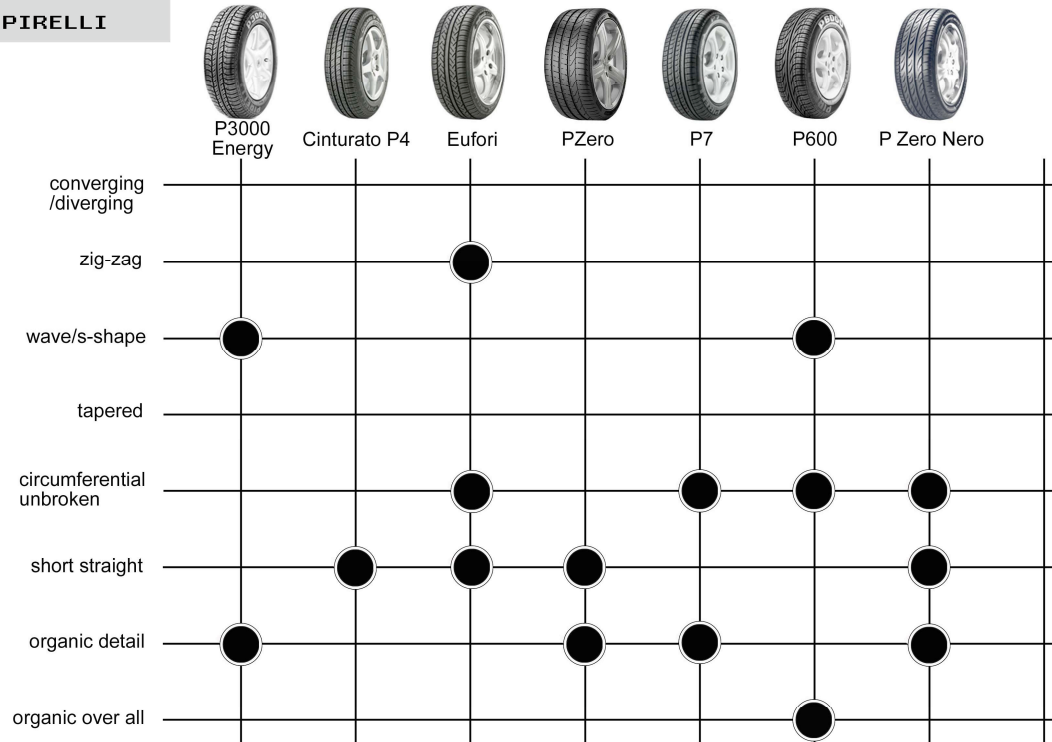
Continental - Firestone - Hankook - Michelin - Nokian - Pirelli

## NOKIAN



Continental - Firestone - Hankook - Michelin - Nokian - Pirelli

## PIRELLI



Continental - Firestone - Hankook - Michelin - Nokian - Pirelli

## Appendix II – Functional matrix and product specification

Ohlsson's matrix as preparation for lining up the product specifications				
	Process	Miljö	Människa	Ekonomi
Alstring (development)	1.1	1.2	1.3	1.4
Framställning (manufacturing)	2.1	2.2	2.3	2.4
Avyttring (retail/trade)	3.1	3.2	3.3	3.4
Brukning (application/utilization)	4.1	4.2	4.3	4.4
Eliminering (elimination/disposal)	5.1	5.2	5.3	5.4

Grey text indicates an area that was not to be considered.

1.1	
1.2	
1.3	
1.4	
2.1	Manufacturing with existing methods
2.2	
2.3	
2.4	Low cost increase for manufacturing tools
3.1	
3.2	
3.3	Attract buyer*
3.4	Low price escalation relative CSC3
4.1	Fulfill mechanical requirements*
4.2	Minimal noise pollution to environment
4.3	Minimal noise for driver
4.4	Reasonable fuel consumption
5.1	
5.2	
5.3	
5.4	
	*More elaborate in the specification itself

Product specification outline				
<b>MF: Distribute contact between tyre and road</b>				
MF = Main Function				
PF = Partial Function				
O/M = Request(O) /Requirement(M)				
	MF	PF	O/M	weighting (0-5)
Technical				
Dry braking	x		M	5
High speed driving	x		M	5
Wet handling	x		M	4
Dry handling	x		M	5
Lifetime		x	O	3
Regular wear		x	O	2
Rolling resistance		x	O	2
Ergonomics				
Comfort		x	O	2
Suitable noise profile		x	O	1
Aesthetics				
Expressions		x	M	4

## Appendix III - Questionnaire

Which expressions/words do you think are best illustrated by the patterns?

To each pattern choose one expression/word from the left box and two from the right box that most closely illustrate the patterns.

**Precise**

**Functionally supreme**

**Safe**

Pick one

**Speedy/fast**

**Clear&shiny**

**Gadgety**

**Hard**

Pick two

	1	2	3	4	5	6
<b>Precise</b>						
<b>Functionally supreme</b>						
<b>Safe</b>						
<b>Speedy/fast</b>						
<b>Clear&amp;shiny</b>						
<b>Gadgety</b>						
<b>Hard</b>						

**Age:**

**Gender:**

**Education:**

**Occupation:**

**Drivers licence:**

**Interest in cars:**

**Interest in technology:**

## Appendix IV – Expression evaluation results

	Precise	Functionally supreme	Safe	Speedy/fast	Clear&shiny	Gadgety	Hard
Pattern1	5	1	4	6	7	4	3
Pattern2	4	2	4	3	2	7	8
Pattern3	4	5	1	7	5	4	4
Pattern4	1	4	5	5	3	8	4
Pattern5	1	4	5	2	2	9	7
Pattern6	3	4	4	3	2	6	8

Grey number indicates intended expression.

